DOI: 10.26599/FSHW.2025.9250675

Contents lists available at SciOpen

Food Science and Human Wellness

journal homepage: https://www.sciopen.com/journal/2097-0765

China Food Publishing Co.

Growth promotion markers and functional metabolomic analysis of co-cultured *Bifidobacterium animalis* subsp. *lactis* HN-3 and *Lacticaseibacillus paracasei* YL-29 in *Elaeagnus moorcroftii* Wall.*ex Schlecht* juice

Yingdi Teng[a1] & Chenxi Wang[a1] , Wenhao Li[a], Yongqing Ni[ab*], Yan Zhang[ab*]

[a] *School of food science and technology, Shihezi University, Road Beisi, Shihezi Xinjiang Province 832003, China.*

[b] *Key Laboratory of Agricultural Product Processing and Quality Control of Specialty (Co-construction by Ministry and Province), School of Food Science and Technology, Shihezi University, Shihezi, Xinjiang 832003, China.*

ABSTRACT: Co-culturing fermentation can improve the bioactivity and metabolic diversity of bacterial strains. In this study, we explored the cooperation between *Bifidobacterium animalis* subsp. *lactis* HN-3 (B.an3) and *Lacticaseibacillus paracasei* YL-29 (L.cp29) by non-targeted metabolomics and prokaryotic transcriptomics analysis. B.an3 and L.cp29 co-culture showed greater growth than the monoculture fermentation through 7 growth regulating metabolic pathways that facilitated the accumulation of monoculture growth-correlated markers, including, raffinose, stachyose, and L-thymidine involved in nucleotide and galactose metabolism. On the other hand, compared to the monoculture fermentation, the significantly enhanced functional activities of the co-culture were associated with 74 and 68 significantly altered metabolites, such as phenylacetaldehyde, succinic acid, and trans-cinnamic acid with antioxidant, anti - inflammatory, and anti-bacterial properties. Overall, this study revealed the cooperative beneficial relationship between B.an3 and L.cp29. It offered novel insights into the co-culture mechanisms, providing a basis for further development of microbial natural products.

Keywords: Co-culture; Growth-promoting; Functional activity; Cooperation; Fermentation

1. Introduction

Probiotics are a type of microorganisms that are widely used for microbial fermentation. They can regulate the intestinal microbiota of the host and grow and metabolize in the food matrix, thereby producing various beneficial metabolites [1]. Of these, *Bifidobacterium animalis* and *Lactobacillus paracasei* are two major probiotics with vital and extensive applications. *Bifidobacterium animalis* is a dominant flora of the intestinal tracts of infants and young children considering that animal and human feces and milk are its primary sources [2]. *B. animalis* , an anaerobic bacterium, its ability to ferment fruits and vegetables is relatively limited [3], but they can be used for fruit and vegetable fermentation if they utilizate readily available substrates that can support their growth during the fermentation process [4]. Some plant oligosaccharides, such as short-chain fission oligosaccharides, serve as prebiotics and encourage

[1] co-first author
*** Corresponding author**.
yanzhangzqgh@shzu.edu.cn; niyqlzu@sina.com

Received 15 January 2025
Received in revised from 11 February 2025
Accepted 22 April 2025

Bifidobacteria growth, which facilitates the successful fermentation of fruits and vegetables [5]. For example, the viable cell count of strains increased, promoted the enrichment and increased the production of antioxidant and other functional substances in *Bifidobacterium* fermentation of blueberry juice [3]. However, the *Bifidobacterium* in a low survival rate limited the number and amount of oligosaccharides in fruits and vegetables that could be used by them [6]. Surprisingly, *L. paracasei* offers a certain advantage in juice fermentation that it can decompose its polysaccharides, oligofructose, and pectin components, which are not easily used by bifidobacteria [7]. *Lactobacillus paracasei* present naturally in plants and can use most of the plant components to promote nutrient release and absorption from fruit juices, thereby improving the nutritional value of fruit juices [8]. For instance, mulberry juice fermentation by *L. paracasei* altered the characteristics of phenolic substances and produced syringic acid, cyanidin-3-O-rutinoside, and quercetin, which exerted antioxidant and anti-inflammatory properties [9]. These functional substances significantly improved the antioxidant capacity of mulberry juice

Co-culturing *B. animalis* and *L. paracasei* can effectively promote their growth through pre-experimentation. In addition, the antioxidant activity of the co-cultured EWSJ was higher than that of the mono-fermented EWSJ. This aspect can is attributable to the better metabolism of components in the EWSJ through co-culture fermentations of the aforementioned two bacteria as co-culturing combines the metabolic advantages of the individual bacteria [10]. This co-culture strategy enhances the characteristic flavor and texture of fermented foods and is an effective and practical approach for promoting substrate bacteriophage survival and substrate metabolism[11]. Additionally, through soluble chemical signals, co-culturing can activate silent genes not expressed in the conventional monocultures, which contributes to the production of new biologically active structures [12]. Although the activation of silenced secondary metabolite genes through co-culture fermentation is accidental and unpredictable, new compounds produced during the co-culture fermentation of the aforementioned two bacteria may reopen biosynthetic pathways in the previously unexplored classes of substances [13]. For example, when compared with *Lactobacillus* fermentation alone, a mixed fermentation of *Lactobacillus* and *Saccharomyces cerevisiae* is more effective in amino acid and carbohydrate metabolism and augments the efficiency to hydrolyze milk protein and lactose [14]. Shuai Guo et al. reported that the unique substance mangiferin is produced through mixed fermentation of *L. casei* and *L. plantarum*[11]. This mixed fermentation allows efficient expression of crucial substances involved in the TCA cycle (citric acid, succinic acid, and succinyl coenzyme A) in the cells. Meanwhile, according to some studies, co-cultured strains activated the Nrf2-signaling pathway in cells and promoted the antioxidant enzyme expression toward alleviating oxidative stress [15]. Moreover, co-culturing with lactobacilli could significantly enhance the fermentation capacity of specific strains and aid the development of new functional yogurts [16]. Briefly, co-culture fermentation augments the characteristic flavor, texture, and functionality of fermented foods while improving the quality and stability of production of these foods [17].

Therefore, the co-culture strategy can possibly ameliorate the problem of bacterial survival in juice fermentation by complementing the bacteria with nutrition and promoting the growth of respective organisms

[9, 15, 17]. Meanwhile, the metabolic cross - talk and molecular mechanisms underlying bacterial synergy, especially multi - omics - driven pathway coordination and strain - specific functional shifts, have remained largely underexplored [18]. Our study fills this gap by systematically correlating transcriptomic remodeling with metabolomic remodeling to elucidate the ways in which co - culturing enhances the probiotic functionality during EWSJ fermentation. To reveal the synergistic and facilitative effect of *B. animalis* subsp. *lactis* HN-3 (B.an3) and *L. paracasei* YL-29 (L.cp29) in EWSJ fermentation, through metabolomics, we comparatively analyzed metabolites produced by different fermentation groups. We also studied in-depth the function of microbial metabolites produced from a metabolic exchange perspective. Furthermore, the microbial metabolites were thoroughly examined from the metabolic exchange standpoint, and the metabolic mechanism of microbes involves in co-culturing was clarified from the molecular biology perspective. The results are believed to augment the effective utilization of probiotics, possess profound implications for developing fermented foods, and support future theoretical research for promoting probiotic growth with plant-derived components. The findings also provide a theoretical basis of producing more natural active molecules, which can be used in the food industry to develop functional foods.

2. Materials and Methods

2.1 Plant materials and bacterial strains

Fully mature fruits of *Elaeagnus moorcroftii* Wall. *ex Schlecht* (length: 15–25 mm) were harvested from the plants grown in Kashgar, Southern Xinjiang Province, China (73°20–79°57 N, 35°20–40°18E). After exposure to a 90℃ water bath for 5 min, EWS was mashed and filtered, and the pH adjusted to 7; the light yellow liquid obtained was *Elaeagnus moorcroftii* Wall. *ex Schlecht* juice (EWSJ) .

B. animalis subsp. *lactis* HN-3 (B.an3) and *L. paracasei* YL-29 (L.cp29) were collected from the technical innovation team of the Microbiology Lab, at Shihezi University. Before use, they were activated twice in de Man, Rogosa and Sharpe (MRS) broth, a nutrient-rich medium containing peptone, yeast extract and glucose, optimized for lactic acid bacteria cultivation [19], under strict anaerobic conditions for 48 h at 37℃.

2.2 Physicochemical characterization of EWSJ in mono- and co-culture fermentation.

2.2.1 Proliferation characteristics

First, the cell suspension of B.an3, L.cp29 and the mix of them (10^8 CFU/mL, 2%(v/v))were incubated separately in yellow EWSJ during 48 h at 37℃. Then, the cell density and bacterial viable counts were evaluated at 0, 12, 24, 36 and 48h to count the live bacteria of them during the fermentation process. The cell density was measured at 600 nm by using a UV-vis spectrophotometer (PERSEE, Beijing, China). The bacterial viable counts was measured by the real-time quantitative. They were chosen for absolute quantification via real - time quantitative PCR (RT - PCR). The specific primers for B.an3 were B4WF (TGACCAGACCATCGCATTGA) and B4WR (TGACCAGACCATCGCATTGA), targeting a 174 - bp fragment. The amplification protocol followed a three - step approach: initial incubation at 50 ℃ for 2 min,

denaturation at 95 ℃ for 2 min, and then 40 cycles consisting of 95 ℃ for 15 s (denaturation), 55 ℃ for 15 s (annealing), and 72 ℃ for 1 min (extension). The melting curve analysis was performed under conditions of 95 ℃ for 1 min, 55 ℃ for 30 s, and 95 ℃ for 30 s. For L.cp29, the specific primers were ParacaseiF (CAACCGTGATGACACTG) and ParacaseiR (CCAACGTTAATCCGGTACTG), with a target fragment of 135 bp. The amplification employed a two - step method: pre - denaturation at 95 ℃ for 2 min, followed by 40 cycles of 95 ℃ for 5 s (denaturation) and 64 ℃ for 35 s (annealing/extension). The melting curve conditions were 95 ℃ for 1 min, 60 ℃ for 1 min, and 95 ℃ for 30 s. The amplification was carried out using the PerfectStart® Uni RT&qPCR Kit, and the primers were synthesized by Shanghai Sangon Biotech Co., Ltd.

2.2.2 Short-chain fatty acid content

Fermented EWSJ (300 μL) was taken into a 2-mL EP tube, to which 1500 μL of ultrapure water was added (1:5 v/v), vortexed for 30 s, centrifuged for 4 min at 5000 pm, 25℃. Then, take 500 μL of the supernatant into a new 2-mL sterile EP tube, to which 100 μL of 25% metaphosphoric acid solution was added, vortexed for 30 s, centrifuged for 15 min at 1500 r/min, 25℃, and then passed through a 0.45-mm aqueous membrane, after which the supernatant was added into a feed vial for gas chromatography (Agilent 7890B) to analyze SCFA in the sample.

2.2.3 Determination of the antioxidant capacity

The antioxidant capacity was measured by scavenging DPPH and ABTS radicals [20]. An aliquot (200 μL) of the fermented juice was added to a test tube containing 800 μL of the diluted ABTS·+ solution, denoted as A_j. The absorbance of this mixture was measured at 734 nm. The control solutions were prepared using 200 μL of distilled water instead of fermented EWSJ, denoted as A_0.

The 2,2-diphenyl-1-picrylhydrazyl (DPPH·) radical scavenger assay was performed according to the previous method with minor modifications. First, 2 mL of fermented EWSJ was mixed with 0.5 mL of 1 mmol/L of the DPPH solution in 95% (v/v) ethanol and 0.5 mL methanol before incubation for 30 min at room temperature in the dark. The absorbance was measured at 517 nm.

2.3 Non-targeted metabolomic analysis

2.3.1 Preparation of samples

Samples (100 μL) were placed in EP tubes and resuspended by vortexing thoroughly with 400 μL of pre-cooled 80% methanol. The sample was then incubated on an ice bath for 5 min and centrifuged at 15,000 x*g* for 20 min at 4℃. The supernatant was diluted with LC-MS grade water to a final concentration of 53% methanol, transferred into a new Eppendorf tube, and centrifuged again at 15000 x*g* for 20 min at 4℃. The resulting supernatant was injected into the UHPLC-MS/MS system for further analysis.

2.3.2 UHPLC-MS/MS analysis

Ultra-high performance liquid chromatography-mass spectrometry/mass spectrometry (Vanquish UHPLC) (Thermo Fisher, Germany) was analyzed with an Orbitrap Q Exactive TMHF mass spectrometer (Thermo Fisher). The samples were injected on a HypesilGold C18 column (100 mm × 2.1 mm, 1.9 μm) with

a linear gradient at a flow rate of 0.2 mL/min for 17 min. The eluents for the positive polarity mode were eluent A (0.1% aqueous formic acid) and eluent B (methanol), and those for the negative polarity mode were eluent A (5 mmol/L ammonium acetate, pH 9.0) and eluent B (methanol). Eluent B (methanol): 2% B, 1.5 min; 2%–85% B, 3 min; 85%–100% B, 10 min; 100%–2% B, 10.1 min; and 2% B, 12 min. Q The ExactiveTM HF mass spectrometer was operated in positive/negative polarity mode, with a spray voltage of 3.5 kV, a capillary temperature of 320℃, a sheath gas flow rate of 35 psi, and an assist gas flow rate of 10 L/min.

2.3.3 Data preprocessing

To ensure data quality, blank samples were run to clean the UHPLC-MS/MS system, pooled QC samples were inserted every 10 injections, and metabolite signals with CV>20% in QC samples were flagged for inspection. Thereafter, raw data files were generated using UHPLC-MS/MS and processed using Compound Discoverer 3.1 (CD3.1, ThermoFisher) for peak alignment, peak picking, and quantitation for each metabolite [21]. The peaks were matched with mzCloud (https://www.mzcloud.org/), mzVault, and MassList database for accurate qualitative and relative quantitative results. These metabolites were annotated using the KEGG database (https://www.genome.jp/kegg/pathway.html), HMDB database (https://hmdb.ca/metabolites), and LIPIDMaps database (http://www.lipidmaps.org/).Differential metabolites were screened based on the criteria of VIP > 1.0, FC > 1.5, or FC < 0.667, and *P* - value < 0.05. The non-targeted metabolomic analysis had six replications.

2.4 Transcriptomic analysis

2.4.1 RNA extraction

B.an3 and L.cp29 were collected culture in EWS, followed by centrifugation to obtain bacterial cells. After washing the bacterial cells with PBS, total RNA was extracted from the cells using the TRIzol Reagent kit (Thermo Fisher Scientific, MA, USA).

2.4.2 cDNA library construction and RNA sequencing

Total RNA was used as an input material for the RNA sample preparations. The mRNA was purified from total RNA using probes to remove rRNA and broken into small fragments by adding a fragmentation buffer. The cDNA libraries were constructed using Illumina's TruSeq™ RNA Sample Preparation protocol with these fragments as the template. The clustering of the index-coded samples was performed on a cBot Cluster Generation System using TruSeq PE Cluster Kit v3-cBot-HS (Illumia) according to the manufacturer's instructions. After cluster generation, the library preparations were sequenced on an Illumina Novaseq platform and 150 bp paired-end reads were generated.

2.4.4 Data quality control

The raw FastQ - format data was first processed by in - house Perl scripts. These scripts used regular expressions to identify and remove reads with adapter sequences or over 5% N - bases. A Phred - score threshold was set: reads with >20% bases below Q20 were discarded. Simultaneously, Q20, Q30, and GC

content of clean data were calculated. Data was deemed high - quality when Q20 > 80%, Q30 > 70%, and GC content was within the species - specific range [22]. The study had three biological replicates. All downstream analyses relied on this high - quality data, ensuring result reliability and reproducibility.

2.4.5 Bioinformatics analysis

RNA-Seq by Expectation–Maximization (RSEM) is a software package for estimating gene and isoform expressions from RNA-Seq data (http://deweylab.github.io/RSEM/), which was employed for calculating the gene or transcript expressions for both single-end and paired-end sequencing data, enabling the comparison of gene expression differences between samples. After obtaining the read counts for genes, DESeq2 is an R package in Bioconductor that performs differential gene analysis based on the negative binomial distribution (http://bioconductor.org/packages/release/bioc/html/DESeq2.html), which was employed for differential gene expression analysis. DESeq2 operates based on the following two criteria: p-adjust <0.05 and |log2FC| ≥1.

For the annotation of differentially expressed genes, Goatools (https://github.com/tanghaibao/GOatools) was employed to perform gene ontology (GO) enrichment analysis on the gene set. Fisher's exact test was used and a GO function was deemed significantly enriched when the adjusted p-value (p-adjust) was <0.05. The Kyoto Encyclopedia of Genes and Genomes (KEGG) enrichment analysis was conducted using the KEGG Orthology-Based Annotation System 2.0 (http://kobas.cbi.pku.edu.cn). The calculation principle for the KEGG pathway enrichment analysis results was akin to that used for the GO enrichment analysis, with the significance threshold set at an adjusted p-value (p-adjust) of <0.05 to identify significantly enriched KEGG pathways [23].

2.5 Statistical analysis

The statistical analysis of the experimental data was conducted using Origin 9.1 software, while one-way analysis of variance (ANOVA) was performed using SPSS 19.0 software. The results are expressed as the mean ± standard deviation (SD). The experiments were performed in triplicate unless otherwise specified. $*P < 0.05$, $**P < 0.01$, $***P < 0.001$, and $****P < 0.0001$ indicate statistically significant differences.

3. Results and Discussion

3.1 Physicochemical properties of EWSJ during mono- and mixed-cultures fermentation

B.an3 and L.cp29 displayed robust growth throughout monoculture fermentations, attaining a viable count of 9.15 and 9.13 Log CFU/g, respectively (Fig. 1A). Meanwhile, the B3L29 co-culture fermentation exhibited an increase; thereby attaining a viable count of 9.17 Log CFU/g. The real-time quantitative results revealed that B3L29 co-culture growth was better than monoculture growth, which attained a viable count of 3.58 Log CFU/mL at 48 h (Fig. 1B). Nevertheless, the real-time quantitative results of B.an3 and L.cp29 monocultures revealed a viable count of only 2.98 and 2.68 Log CFU/mL at 48 h, respectively. Similarly, cherry silverberry juice was fermented with monocultures and co-cultures of *L. plantarum* and *L. casei*;, the

growth of co-culture was better than that of monoculture [24]. However, the viable counts exceeded the standard count for commercial probiotic fermented food production (10^7 Log CFU/mL) [25].

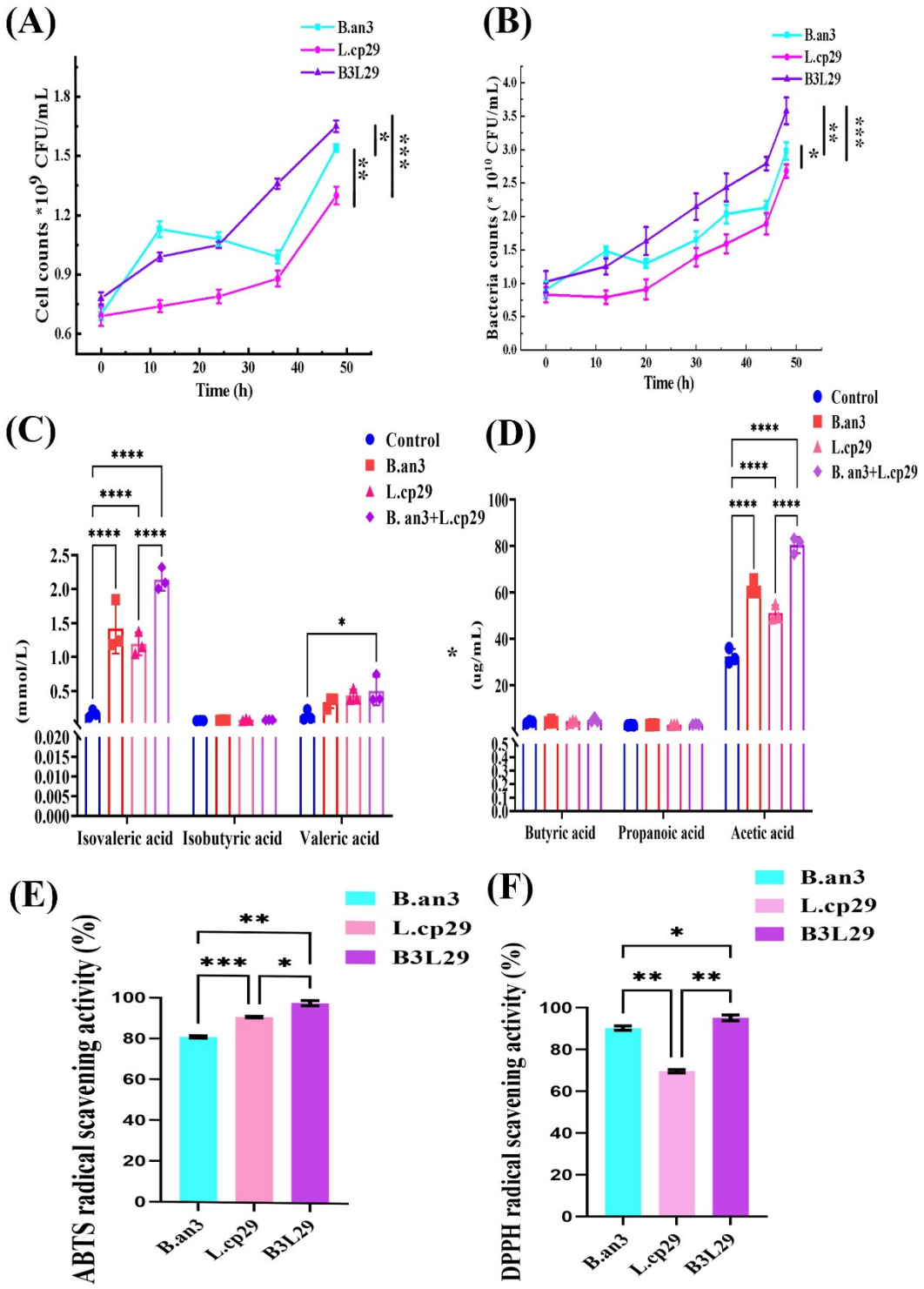

Fig 1: (A) The dynamics of viable counts in (B.an3, L.cp29, and B3L29) fermented by *Bifidobacterium animalis* subsp. *lactis* HN-3, *Lacticaseibacillus paracasei* YL-29, and co-culture-fermented *Elaeagnus moorcroftii* Wall.*ex Schlecht* juice (EWSJ) during 48 h; (B) The bacterial counts in mono-cultures and co-culture via spread plate method; (C) and (D) the determination of short-chain fatty acids (Isovaleric acid, isobutyric acid, valeric acid, butyric acid, propionic acid and acetic acid) in EWSJ before and after mono- and mixed-cultures fermentation; antioxidant activity assays (E) ABTS and (F) DPPH-free radical scavenging activity of B.an3, L.cp29, and co-culture-fermented EWSJ at 48 h. Values represent averages of triplicate measurements. Data is expressed as the mean ± SD. Asterisks illustrate statistical significance. *$P < 0.05$, **$P < 0.01$, ***$P < 0.001$.

In addition, we determined the content of short-chain fatty acids in EWSJ after mono- and co-culture fermentation. As shown in Figures 1C and 1D, the highest content of acetic acid was detected in EWSJ after B.an3 and L.cp29 fermentation alone, which were 60.18 and 49.45 ug/mL, respectively. Meanwhile, after co-culture fermentation, the content of acetic acid was also the highest (81.78 ug/mL). When compared to the mono-culture fermentation, after co-culture fermentation, the content of both acetic acid and isobutyric acid increased significantly by 32.33 ug/mL and 0.009 mmol/L, respectively. Consequently, it indicated that the content of short-chain fatty acids in EWSJ could be improved after co-culture fermentation than after mono-culture fermentation. Acetic acid and isobutyric acid can be used as carbon sources to promote the growth of strains as well as the main metabolites to effectively inhibit inflammation and reduce damage caused by oxidative stress [26]. Hence, the increase in their contents could further enhance the functional activity of EWSJ after fermentation.

We also evaluated the influence of fermentation on the antioxidant properties of EWSJ in terms of ABTS and DPPH-radical scavenging activities. Figures 1E and 1F illustrate the improvement in the antioxidant activities of EWSJ fermented using the B3L29 co-culture compared with monocultures. The antioxidant potential of co-culture fermentation was significantly higher (ABTS: 98.12 ± 1.26 and DPPH: 95.18 ± 1.4) than that of monoculture fermentations (B.an3: ABTS: 80.98 ± 0.53 and DPPH: 90.22 ± 1.04; L.cp29: ABTS: 91.06 ± 0.33 and DPPH: 69.59 ± 0.8).

Overall, co-culture fermentation resulted in a high probiotic density and antioxidant activity, which signifies the synergistic effects of B.an3 and L.cp29 and the production of unique/enhanced metabolites with higher bioactivities or functional properties through co-culture [11]. However, the mechanism underlying the strain–substrate interaction leading to these results remains unclear. Therefore, the metabolites of monoculture and co-culture fermentations were analyzed through metabolomic analyses.

3.2.2 Differential metabolites and major metabolism

3.2.2.1 Differential metabolites and major metabolism between the BL versus B group

74 differential metabolites in the EWSJ of the BL versus B group included 9 carbohydrates, 5 amino acids, 8 fatty acids, 8 terpenoids, 6 benzenoids, 5 pyrimidines, 2 carboxylic acids, 7 steroids, 2 indoles, 1 purine, and 21 others. Amino acids, fatty acids, and benzenoids were the major contributors in the BL versus B group (Figs. 2e-f). Notably, the number of upregulated metabolites of amino acids, pyrimidines, and steroids exceeded the number of downregulated metabolites. This observation demonstrated that the strains converted other metabolite classes into structures of functionally active components, which resulted in higher functional activity [27]. Conversely, the levels of carbohydrates and purine were decreased during fermentation, suggesting that the strains used and converted these metabolites to promote bacterial growth and energy production [28].

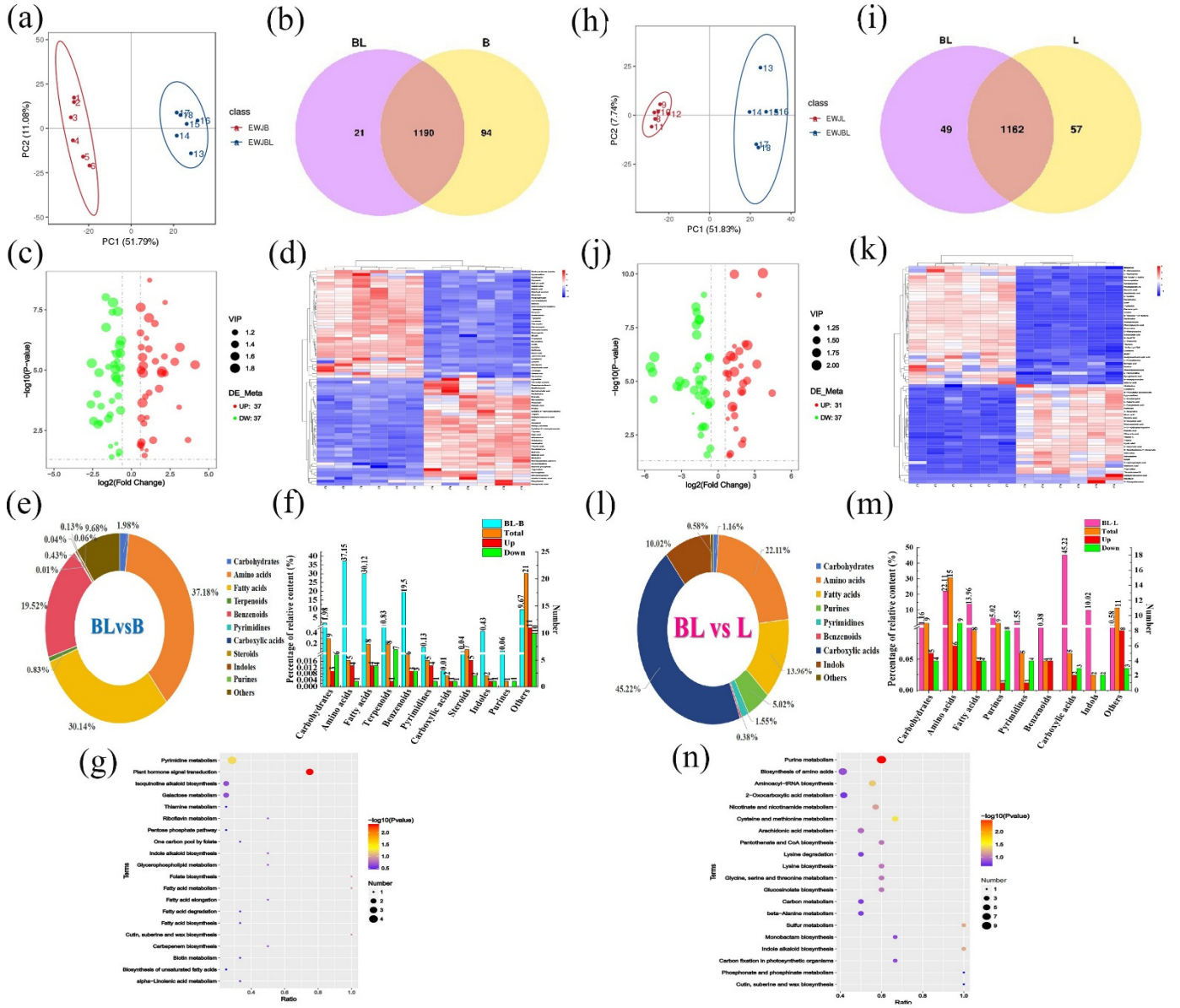

Fig 2: The profiles of differential metabolites from *Bifidobacterium animalis* subsp. *lactis* HN-3, *Lacticaseibacillus paracasei* YL-29, and co-culture-fermented *Elaeagnus moorcroftii* Wall.*ex Schlecht* juice (EWSJ) samples. The principal component analysis (PCA) of metabolic profiles in BL versus B (a) and BL versus L (h) fermented EWSJ samples (six biological replication) based on the metabolomic dataset; Venn diagram of the differential metabolites of BL versus B (b) and BL versus L (i) fermented EWSJ; the V-plot of BL versus B (c) and BL versus L (j) fermented EWSJ; the heat map of differential metabolites in BL versus B (d) and BL versus L (k) fermented EWSJ; the classes of differential metabolites of BL versus B (e) and BL versus L (l) fermented EWSJ; (f) the numbers and percentages of relative content of carbohydrates, amino acids, fatty acids, terpenoids, benzenoids, pyrimidines, carboxylic acids, steroids, indoles, purine, and others in BL versus B fermented EWSJ; (m) the numbers and percentages of relative content of carbohydrates, amino acids, fatty acids, terpenoids, benzenoids, pyrimidines, carboxylic acids, steroids, indoles, purine, and others in BL versus L fermented EWSJ; the Bubble diagram of differential metabolic pathways in BL versus B (g) and BL versus L (n) fermented EWSJ. Data is expressed as the mean ± SD.

Following comparison with the KEGG database, 4 metabolic pathways were illustrated (Fig. 2g). The enriched KEGG pathways were predominantly related to metabolism, which included "pyrimidine metabolism," "isoquinoline alkaloid biosynthesis," "galactose metabolism," and "thiamine metabolism." The metabolites associated with these metabolic pathways were primarily amino acids, nucleotides, and carbohydrates, which played vital roles in bacterial growth and cell formation [29]. According to Wu J et al., the homologous resistance and cross-resistance of *L. plantarum* L1 and *L. plantarum* L2 significantly

upregulated genes related to membrane transport, amino acid metabolism, nucleotide metabolism, and cell growth [30].

3.2.2.3 Differential metabolites and major metabolism between the BL versus L group

In total, 68 differential metabolites were identified in the EWSJ of the BL versus L group, including 9 carbohydrates, 15 amino acids, 8 fatty acids, 9 purines, 5 pyrimidines, 4 benzenoids, 5 carboxylic acids, 2 indoles, and 11 others. The top five classes of differential metabolites were carboxylic acids, amino acids, fatty acids, indols, and purines (Figs. 2l-m). Notably, the number of downregulated metabolites exceeded that of upregulated metabolites of amino acids, purines, pyrimidines, carboxylic acids, and indols. This finding indicated that the strains used and converted these metabolites to promote cell growth and energy production [31]. On the other hand, the number of upregulated metabolites surpassed the number of downregulated metabolites of carbohydrates and benzenoids. These metabolites contributed to strain growth and enhanced their functional activity [28].

The differential metabolites were involved in the metabolic pathways (Fig. 2n) such as “purine metabolism,” “amino acid biosynthesis,” “aminoacyl-tRNA biosynthesis,” “2-oxocarboxylic acid metabolism,” “nicotinate and nicotinamide metabolism,” “cysteine and methionine metabolism,” and “arachidonic acid metabolism.” The metabolites predominantly associated with these metabolic pathways are amino acids, purines, carboxylic acids, and nucleotides. Moreover, among these classes of metabolites, amino acids, purines, and carboxylic acids were all downregulated, which meant that the levels of these three metabolites decreased considerably because of strain growth and metabolism [32]. For instance, the downregulated uracil was indirectly related to the upregulated L-thymine. However, uracil as a key pyrimidine in pyrimidine metabolism increases the *L. plantarum* growth rate and the production of an antimicrobial substance by these bacteria. Also, uracil’s involvement in RNA synthesis and antimicrobial production supports microbial growth and competitive fitness in host environments [33]. The aforementioned results indicate that the essential role of B.an3 in co-culture was to promote bacterial growth.

3.3 Growth-promoting markers and corresponding transformation pathways

3.3.1 Growth promotion of B.an3 in the B3L29-fermented EWSJ compared with the B.an3-fermented EWSJ

Through the KEGG database analysis, the pathways of potential mechanisms underlying the effects of components in the BL versus B group on bacterial growth were elucidated (Fig. 3). Carbohydrates, benzenoids, fatty acids, indoles, pyrimidines, and amino acids promoted strain growth (Fig. 3A), including stachyose, raffinose, L-asparagine, jasmonic acid, salicylic acid, L-thymidine , indole-3-acetic acid, and riboflavin. Raffinose, a carbohydrate, serves as a substrate for microbial fermentation. As a key energy source, it powers bacterial replication and enzyme synthesis, promoting strain growth [34]. L-asparagine’s role in nitrogen metabolism and amino acid biosynthesis supports microbial growth and metabolic adaptability [35]. Jasmonic acid signals in bacteria, regulating stress responses, defense, secondary metabolite production, and inducing growth - and adaptation - related gene expression for better fermentation - environment survival [36]. Salicylic acid safeguards fermentation systems against pathogens with its antimicrobial properties and

regulates genes for bacterial growth as a signaling molecule [37]. Indole-3-acetate acts as a microbial signaling molecule, regulating bacterial gene expression. This modulation affects biofilm formation, virulence factor production, and inter - bacterial communication, ultimately promoting strain growth and adaptability in the fermentation environment [38].Riboflavin forms key coenzymes FAD and FMN, which drive redox reactions in bacteria. These reactions fuel energy production, macromolecule biosynthesis, and antioxidant defense, all of which support bacterial growth [39].

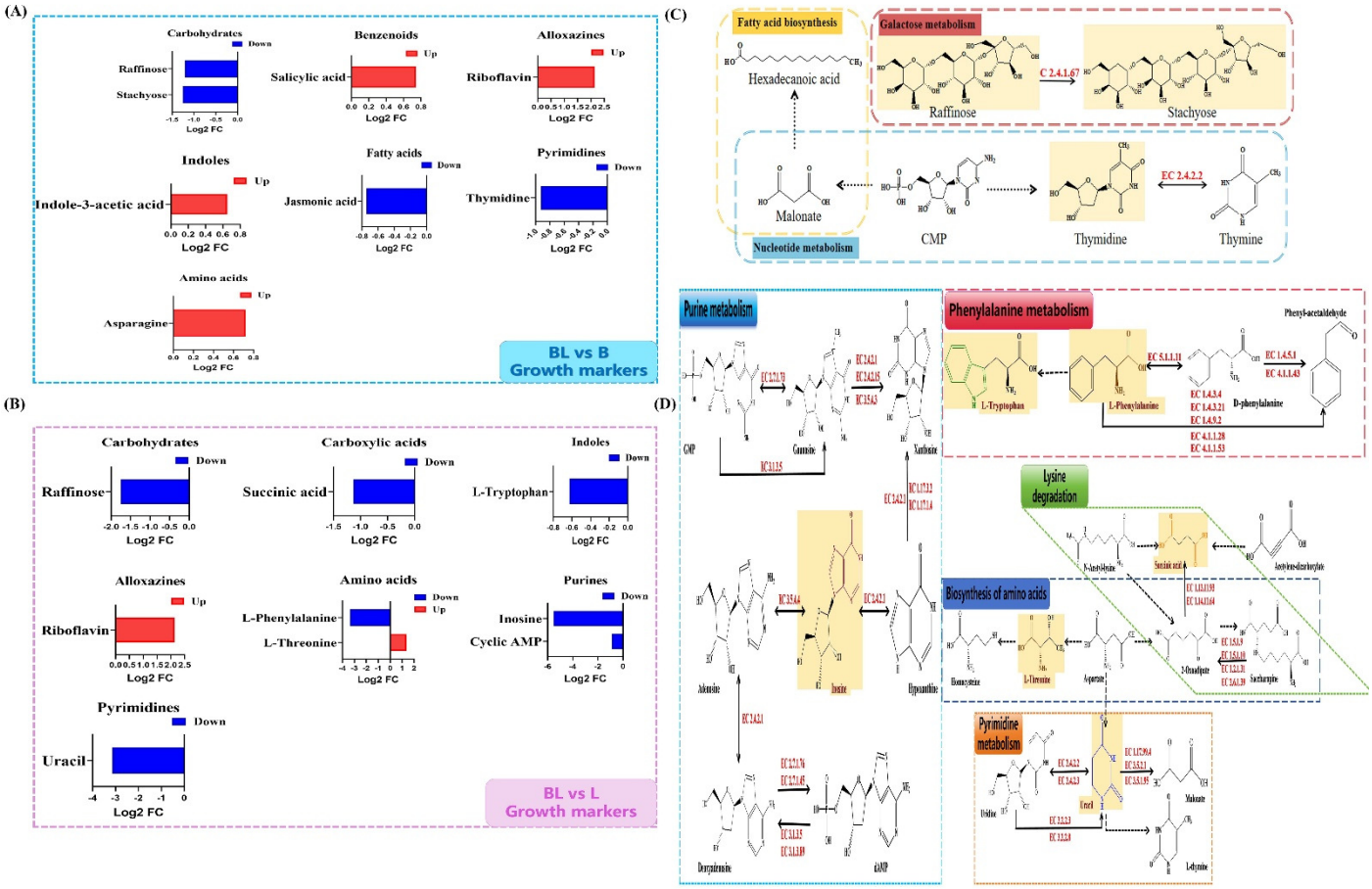

Fig 3: The integration map of the important metabolic pathways on bacterial growth. Up- and downregulation of growth markers during the BL versus B (A) and BL versus L (B) fermentation; the potential metabolic pathway of the effect on bacterial growth during the BL versus B (C) BL versus L(D) fermentation; The red color represents upregulation and blue color represents downregulation. The full line represents direct conversion and the dotted line represents indirect conversion.

These classes of metabolites were primarily involved in nucleotide metabolism, fatty acid biosynthesis, and galactose metabolism (Fig. 3C). The pyrimidine - nucleoside phosphorylase (EC 2.4.2.2) catalyzes the conversion of raffinose to stachyose. This conversion provides an alternative energy - storage form and modulates bacterial metabolic pathways, potentially influencing the production of bioactive metabolites that enhance fermentation system functionality. Additionally, this enzyme converts various functional groups into nucleoside structures, and thus can potentially be used as a diagnostic or therapeutic agent [40]. Nucleotide metabolism included pyrimidine metabolism and purine metabolism. The downregulated L-thymidine exhibited a direct or indirect translational relationship with upregulated CMP and thymine. As a key pyrimidine - metabolism metabolite, L - thymidine is vital for bacterial DNA synthesis, ensuring genome replication and repair for cell division and growth, and regulating nucleotide metabolism to maintain cell

integrity and function [41]. Notably, two direct conversions were observed in the BL versus B group and were two transfer reactions. The enzyme predicted for the precursor L-thymidine was galactinol-raffinose galactosyltransferase (EC 2.4.1.67).

3.3.2 Growth promotion of L.cp29 in the B3L29-fermented EWSJ compared with the L.cp29-fermented EWSJ

Based on metabolite regulation and KEGG metabolic pathway analyses, the effects of change in the differential metabolites of the BL and L group on bacterial growth were investigated (Fig. 3). In total, this group had 7 classes of metabolites, namely carbohydrates, carboxylic acids, indoles, alloxazines, amino acids, purines, and pyrimidines, which promoted strain proliferation and growth (Fig. 3B). Furthermore, 4 metabolites, namely L-phenylalanine, L-threonine, inosine, and adenosine 3',5'-cyclic phosphate (cyclic AMP), from among amino acids and purines exhibited plant growth-growth promoting activity and serve as metabolic signal molecules regulating strain growth and metabolism. L-phenylalanine's function as a metabolic signaling molecule underscores its role in coordinating microbial-plant interactions and growth regulation [42]. L-threonine's contribution to cell membrane integrity and protein synthesis underscores its importance in microbial proliferation [43]. Inosine's role in nucleotide salvage pathways supports energy metabolism and microbial survival under nutrient-limited conditions [44]. cAMP's function as a secondary messenger mediates microbial responses to environmental stressors, influencing biofilm formation and virulence [45].

To further explore changes in these classes of metabolites, we comprehensively analyzed 24 differential metabolites involved in 5 metabolic pathways, namely purine metabolism, phenylalanine metabolism, lysine degradation, amino acid biosynthesis, and pyrimidine metabolism (Fig. 3D). We have summarized these biotransformation reactions and their regulation, and predicted the enzymes involved in metabolite transformation in Figure 3d. The enzymes predicted for the product inosine were adenosine deaminase (EC 3.5.4.4) and purine-nucleoside phosphorylase (EC 2.4.2.1). Phenylalanine racemase (EC 5.1.1.11), an isomerase, catalyzes the conversion of L-phenylalanine to D-phenylalanine. This enzyme can be produced by *L. plantarum* [46]. In addition, L-phenylalanine is converted to phenyl-acetaldehyde by the action of aromatic-L-amino-acid decarboxylase (EC 4.1.1.28) and phenylalanine decarboxylase (EC 4.1.1.53). The reduction enzymes 2-oxoadipate dioxygenase (EC 1.13.11.93) and glutarate dioxygenase (EC 1.14.11.64) were predicted to transform the product succinic acid. This reaction establishes a critical link between succinic acid and redox metabolism, thereby facilitating energy production in microbial systems. However, the hydrolytic enzymes uridine nucleosidase (EC 3.2.2.3) and ribosylpyrimidine nucleosidase (EC 3.2.2.8) were predicted to catalyze the conversion of the precursor uridine to uracil, thereby promoting strain growth [47]. Uridine's role in nucleotide salvage pathways ensures microbial survival by recycling nucleosides for RNA biosynthesis [48].

Overall, the downregulation of carbohydrates and carboxylic acids, indoles, purines, and pyrimidines was hypothesized to indicate that these components were consumed and used during *Lactobacillus* growth, leading to their conversion to other substances.

3.4 Function-promoting substances and corresponding transformation pathways

3.4.1 Function promotion and transformation pathways in the co-culture-fermented EWSJ compared with B.an3-fermented EWSJ

Some differential metabolites produced during fermentation had different structures and thus exhibited different functional activities, such as antioxidant, anti-inflammatory, antitumor, and antibacterial. Among these metabolites, CMP has a phosphate group and ribose group, which are involved in DNA and RNA synthesis as well as in the repair of cells; CMP's involvement in nucleic acid biosynthesis and cellular repair processes underscores its essential role in microbial proliferation and functional activity. Hence, they are crucial for cell proliferation and growth [49]. Deoxyuridine 5'-phosphate is a deoxyribonucleotide with a structure that can affect DNA synthesis and repair, which thus inhibits tumor cell proliferation. dUMP's structural properties enable its inhibitory effects on DNA synthesis, positioning it as a key metabolite in antitumor and antimicrobial strategies.

However, during fermentation, metabolic transformation results in the conversion of these metabolites into each other, leading to structural changes in bioactive components (Fig. 4A). In pyrimidine metabolism, CMP and dUMP are generated, both of which possess the nucleobase cytosine, pentose ribose, and phosphate groups, and thus exert antimicrobial and antitumor effects. L-asparagine as a precursor substance is converted to glutamate, which decreases its content.

In conclusion, functional activities, such as anticancer and antitumor activities, of the co-culture improved when compared with those of the B.an3-fermented EWSJ.

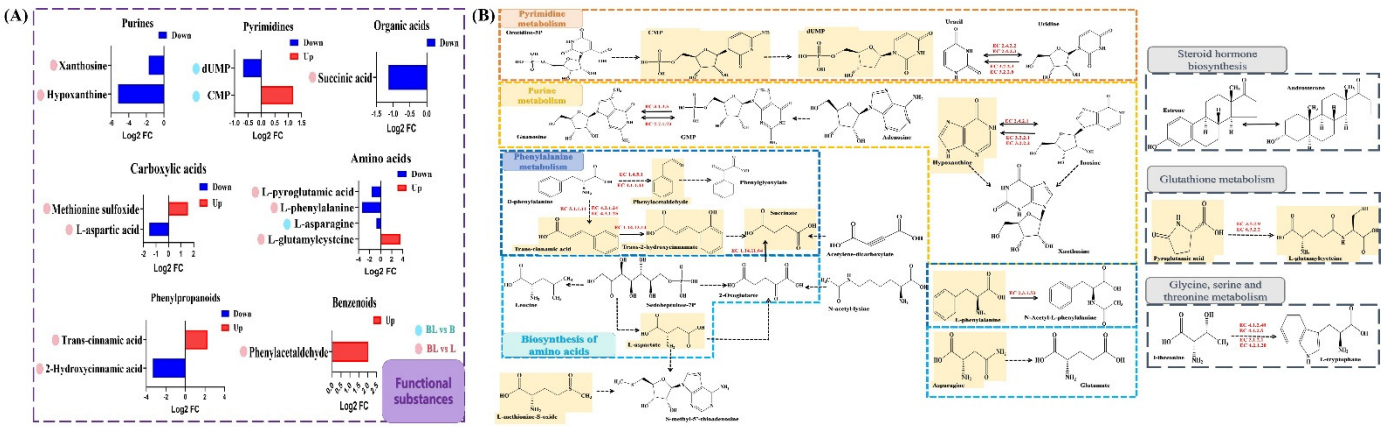

Fig 4: The integration map of functional metabolites on the important metabolic pathways. (A) Up- and downregulation of functional metabolites in co-culture and mono-culture fermentations; (B) the potential mechanisms pathway of the effect on functional metabolites after co-culture and monoculture fermentation. The red color represents upregulation and blue color represents downregulation. The full line represents direct conversion and the dotted line represents indirect conversion.

3.4.2 Function promotion and transformation pathways in the co-culture-fermented EWSJ compared with the L.cp29-fermented EWSJ

Eleven functional substances were classified as purines, organic acids, carboxylic acids, amino acids, phenylpropanoids, and benzenoids (Fig. 4A). Figure 4B presents the corresponding metabolic pathways in which these metabolites are involved. The enzymes D-amino acid dehydrogenase (EC 1.4.5.1) and

phenylpyruvate decarboxylase (EC 4.1.1.43) were predicted to transform the precursor substance D-phenylalanine into the upregulated phenylacetaldehyde, which triggered an increase in antioxidant, anti-inflammatory, and antimicrobial activities [50]. This metabolic conversion underscores the significance of phenylacetaldehyde in potentiating the antimicrobial, anti-inflammatory and antioxidative properties of probiotic consortia. In addition, this biosynthetic pathway highlights L-phenylalanine's contribution to the production of antimicrobial metabolites via D-phenylalanine intermediates. Similarly, the enzymes phenylalanine racemase (EC 5.1.1.11) and phenylalanine ammonia-lyase (PAL) (EC 4.3.1.24 and EC 4.3.1.25) were predicted to act on D-phenylalanine and trans-cinnamate, which increased the content of trans-cinnamic acid. Trans-cinnamic acid's antimicrobial properties highlight its role in probiotic defense mechanisms against pathogenic microbes [51]. Moreover, trans-cinnamate 2-monooxygenase (EC 1.14.13.14) is an enzyme predicted to act on trans-cinnamic acid and 2-hydroxycinnamate. The enzyme glutarate dioxygenase (EC 1.14.11.64) was predicted to act on 2-oxoglutarate and succinate. Both trans-cinnamate 2-monooxygenase and glutarate dioxygenase acted as oxidoreductases. The products trans-2-hydroxycinnamate and succinic acid, respectively, exhibited better antioxidant activity than their precursors [52]. This enzymatic transformation underscores the pivotal role of 2-hydroxycinnamate in augmenting antioxidant capacity via redox modulation [53]. Succinic acid's dual involvement in energy metabolism and antioxidant defense highlights its multifaceted role in microbial co-culture dynamics [54]. Meanwhile, purine nucleosidase (EC 3.2.2.1) and inosinase (EC 3.2.2.2) are the hydrolytic enzymes predicted to act on inosine and hypoxanthine. Succinic acid's dual involvement in energy metabolism and antioxidant defense highlights its multifaceted role in microbial co-culture dynamics, and it also shows antibacterial effects [55]. However, N-acetyltransferase (EC 2.3.1.53) converted L-phenylalanine to N-acetylphenylalanine. Pyroglutamase (EC 3.5.2.9) and gamma-glutamyl-L-cysteine synthetase (EC 6.3.2.2) catalyzed the conversion of the downregulated pyroglutamic acid to the upregulated L-glutamylcysteine, thereby improving the antioxidant activity. This enzymatic conversion replenishes intracellular glutathione pools, thereby fortifying cellular defenses against oxidative stress. Pyroglutamic acid serves as a metabolic reservoir for glutathione biosynthesis, particularly under oxidative stress conditions.

Consequently, through transformation reactions, the co-culture improved the functional activities of antitumor, antioxidant, antibacterial, and antitumor activities compared with those of L.cp29-fermented EWSJ.

Overall, the increase in the bioactivity of fermented EWSJ was hypothesized to be caused by the alteration of enzymes produced by the strain. The different classes of differential metabolites exhibited varied structures, which resulted in the production of different products with distinct functional activities. For instance, amino acids containing sulfhydryl or hydroxyl groups served as natural antioxidants as they inactivated free radicals through resonance delocalization on the entire phenolic ring structure [56]. Pyrimidine is a diazine with two nitrogens at the 1- and 3-positions and exerts antitumor and anti-inflammatory effects

[57]. In addition, the purine molecular structure consists of fused pyrimidine and imidazole rings, which possess antioxidant and anti-inflammatory properties [58].

3.5 Transcriptome comparison of fermented EWSJ of B3L29, B.an3 and L.cp29

3.5.1 Transcriptomic data assembly, quality assessment, and annotation

To investigate the gene expression of B3L29, B.an3 and L.cp29 fermented on EWSJ, and the RNA was extracted and subjected to transcriptome sequencing. Overall, 7647202 ± 258453, 7862612 ± 124332, and 7313849 ± 293535 reads were detected in B3L29, B.an3, and L.cp29 groups, respectively; the Q30 values of all samples were higher than 97% (Table S3). The PCA plots revealed a considerable divergence among BLB, BG, and BF and BLL, LG, and LF, respectively (Figs. 5a and 5g). The correlation matrix was used to analyze the correlation among BLB, BG, and BF and BLL, LG, and LF, respectively, rvealing high correlation coefficients (> 0.9 and > 0.93) that met the criteria for transcriptomic analysis (Figs. 5b and 5h).

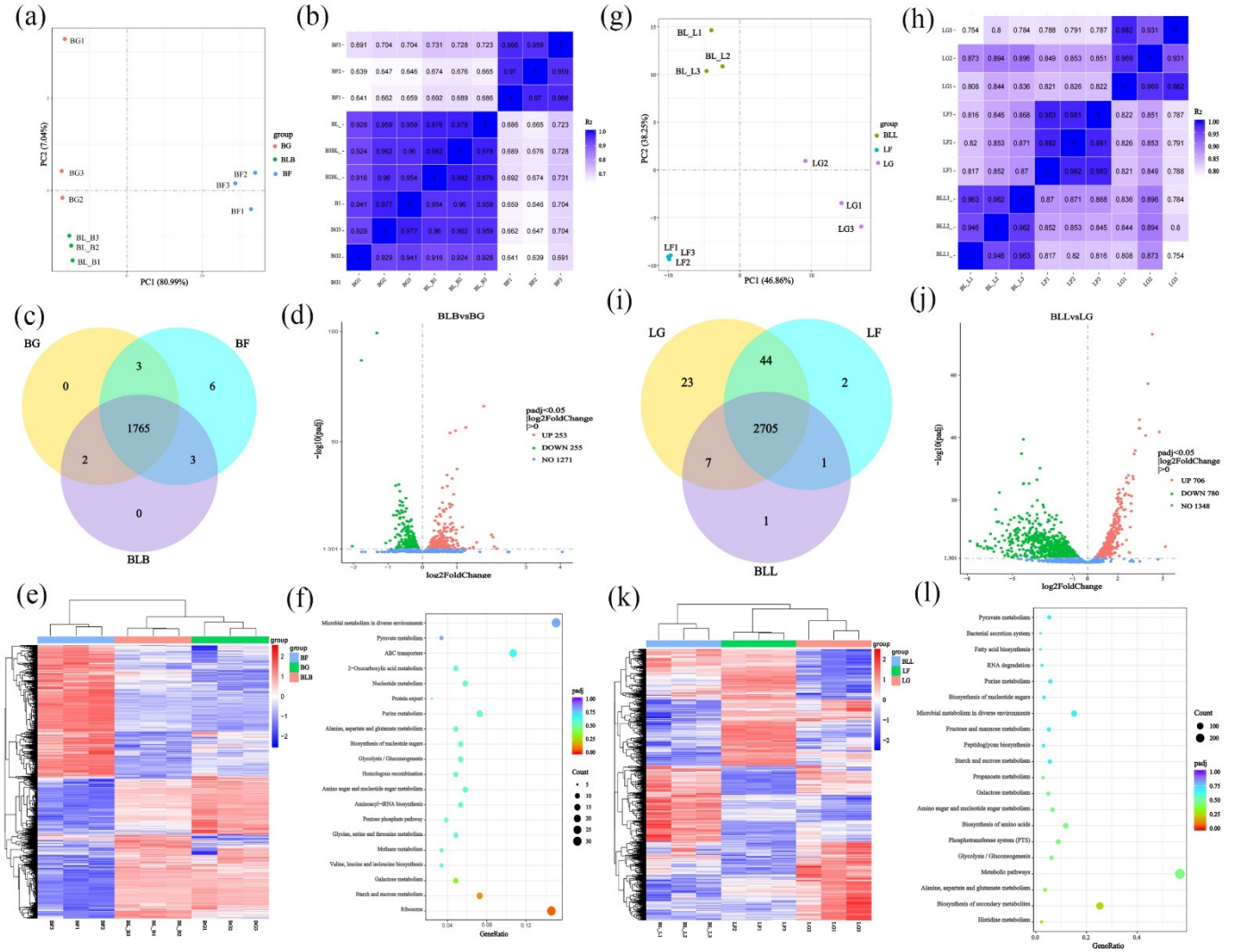

Fig 5: The profiles of differential genes from *Bifidobacterium animalis* subsp. *lactis* HN-3, *Lacticaseibacillus paracasei* YL-29, and co-culture-fermented *Elaeagnus moorcroftii* Wall.*ex Schlecht* juice (EWSJ) samples. The principal component analysis (PCA) of metabolic profiles in BL versus B (a) and BL versus L (g) fermented EWSJ samples (six biological replication) based on transcriptomic dataset; the correlation heat map of differential genes of BL versus B (b) and BL versus L (h) fermented EWSJ; Venn diagram of the differential metabolites of BL versus B (c) and BL versus L (i) fermented EWSJ; the V-plot of BL versus B (d) and BL versus L (j) fermented EWSJ; the heat map of differential genes in BL versus B (e) and BL versus L (k) fermented EWSJ; the Bubble diagram of differential metabolic pathways in BL versus B (f) and BL versus L (l) fermented EWSJ. Values represent averages of triplicate measurements. Data is expressed as the mean ± SD.

3.5.2 Expression analysis of differentially expressed genes (DEGs) and KEGG enrichment

To better investigate the differences in the transcriptional level, DEGs between BLB vs BG vs BF and BLL vs LG vs LF groups were compared and acquired a total of 1779 and 2783 DEGs, respectively (Figs. 5c and 5i). There were 253 upregulated and 255 downregulated DEGs in BLB vs BG vs BF comparison; 706 upregulated and 780 downregulated DEGs in BLL vs LG vs LF comparison (Figs. 5d and 5j). The expression heatmaps of DEGs before and after mono-culture fermentations and after co-culture fermentation illustrated significant differences in the expression of differential genes (Figs. 5e and 5k). With the reference to the KEGG database, DEGs were annotated, and pyruvate metabolism, purine metabolism, and microbial metabolism in diverse environments were found to be the most enriched pathways between co-culture and mono-culture comparisons (Figs. 5f and 5l), highlighting the importance of these DEGs in co-culture and mono-culture fermentations of EWS.

To verify the accuracy of the transcriptome data, 28 DEGs were selected and validated using real-time fluorescence quantification (Qrt-PCR). The results showed that the qRT-PCR gene expression trends were generally consistent with the transcriptome expression trends, indicating that the transcriptome data were valid and reliable (Fig. S5).

3.5.3 Analysis of the enzymes and differential metabolites related to growth promotion and function promotion in EWSJ

3.5.3.1 Growth and function promotions of B.an3 in the B3L29-fermented EWSJ compared with the B.an3-fermented EWSJ

Based on KEGG enrichment analysis and gene function annotated DEGs, BLC1_RS07585 was highly expressed at BG, and BLC1_RS07880 (MsmE), BLC1_RS07890, BLC1_RS06765 (NudC), and BLC1_RS01105 (TmK) were highly expressed at BLB (Figs. 6a-b). Only one transformation was related to growth promotion, that is, stachyose to raffinose. The expression of BLC1_RS07890 in BG was significantly upregulated, which led to the downregulation of stachoyse (Figs. 6c-d). Therefore, transformations of differential metabolites related to bacterial growth in the BL and B group involved only a single transfer reaction. The decrease in the raffinose and stachyose levels as prebiotics indicated their utilization for bifidobacterial growth [59]. Two transformation reactions were observed in function promotion, which were regulated by BLC1_RS07890 and MsmE. The expression of these two DEGs were significantly decreased in BLB, causing the downregulation of raffinose (Figs. 6e-f). Raffinose has anti-obesity and anti-diabetic effects and prevents non-alcoholic fatty liver disease by inhibiting lipid accumulation [60].

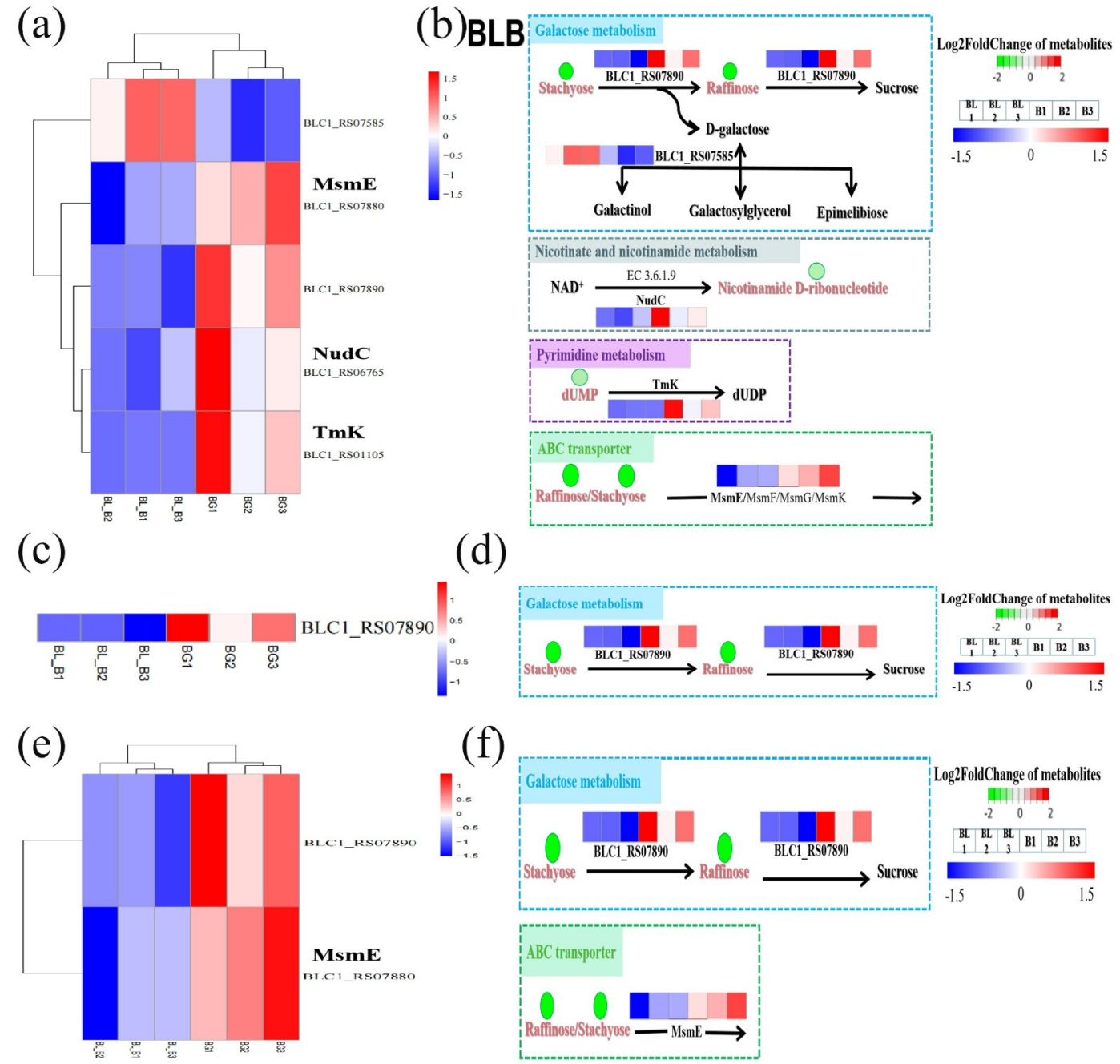

Fig 6: Schematic diagram depicting the backbone pathways for the biosynthesis of several bioactive compounds and the expression of key genes in BL versus B. The heatmap shows the level of gene expression (calculated using Log_2Fold Change, based on transcriptome data) (a), differential genes expression associated with bacterial growth (c) and functional activity (e) from red (higher expression) to blue (lower expression); the backbone pathways for the biosynthesis of several bioactive compounds and the expression of key genes (b), metabolic pathways associated with bacterial growth (d) and functional activity (f). The red color represents upregulation and blue color represents downregulation.

3.5.3.2 Growth and function promotions of L.cp29 in the B3L29-fermented EWSJ compared with that in the L.cp29-fermented EWSJ

As shown in Figure 7a, 33 DEGs regulating key enzymes were screened, of which 18 genes were significantly upregulated in LG and 17 were significantly upregulated in BLL. According to KEGG enrichment analysis and gene function annotated DEGs, raffinose, L-aspartate, GMP, and L-cysteine served as vital metabolites in different metabolic pathways (Fig. 7b). L-aspartic acid's involvement in nitrogen

assimilation and nucleotide biosynthesis supports microbial growth and immune modulation [61]. HKJ34_RS10985 and HKJ34_RS04435 were highly expressed in BLL, and HKJ34_RS08535 (PyrR), HKJ34_RS04950 (TdcB), and HKJ34_RS00370 (TrpB) were highly expressed in LG (Fig. 7c). Meanwhile, succinate and uracil acted as the central metabolites of lysine degradation and pyrimidine metabolism that improved bacterial growth (Fig. 7d) [33, 62]. There were 6 metabolic pathways related to function promotion, and 4 DEGs were significantly increased in LG and 5 DEGs were significantly increased in BLL (Fig. 7e). In the LG group, the high expression of HKJ34_RS04435 and HKJ34_RS10985 resulted in the downregulation of succinate and raffinose. Meanwhile, in the BLL group, the high expression of HKJ34_RS03190 (Hpt) and HKJ34_RS07195 (Args) resulted in the downregulation of hypoxanthine and L-arginine, respectively; the downregulation of HKJ34_RS01735 (UlaA) and HKJ34_RS14350 (UlaC) expression led to the accumulation of L-ascorbate (Fig. 7f), which may have contributed to alleviating the constipation symptoms [63]. L-ascorbate's antioxidant activity contributes to gut health by scavenging reactive oxygen species and supporting epithelial integrity [64].

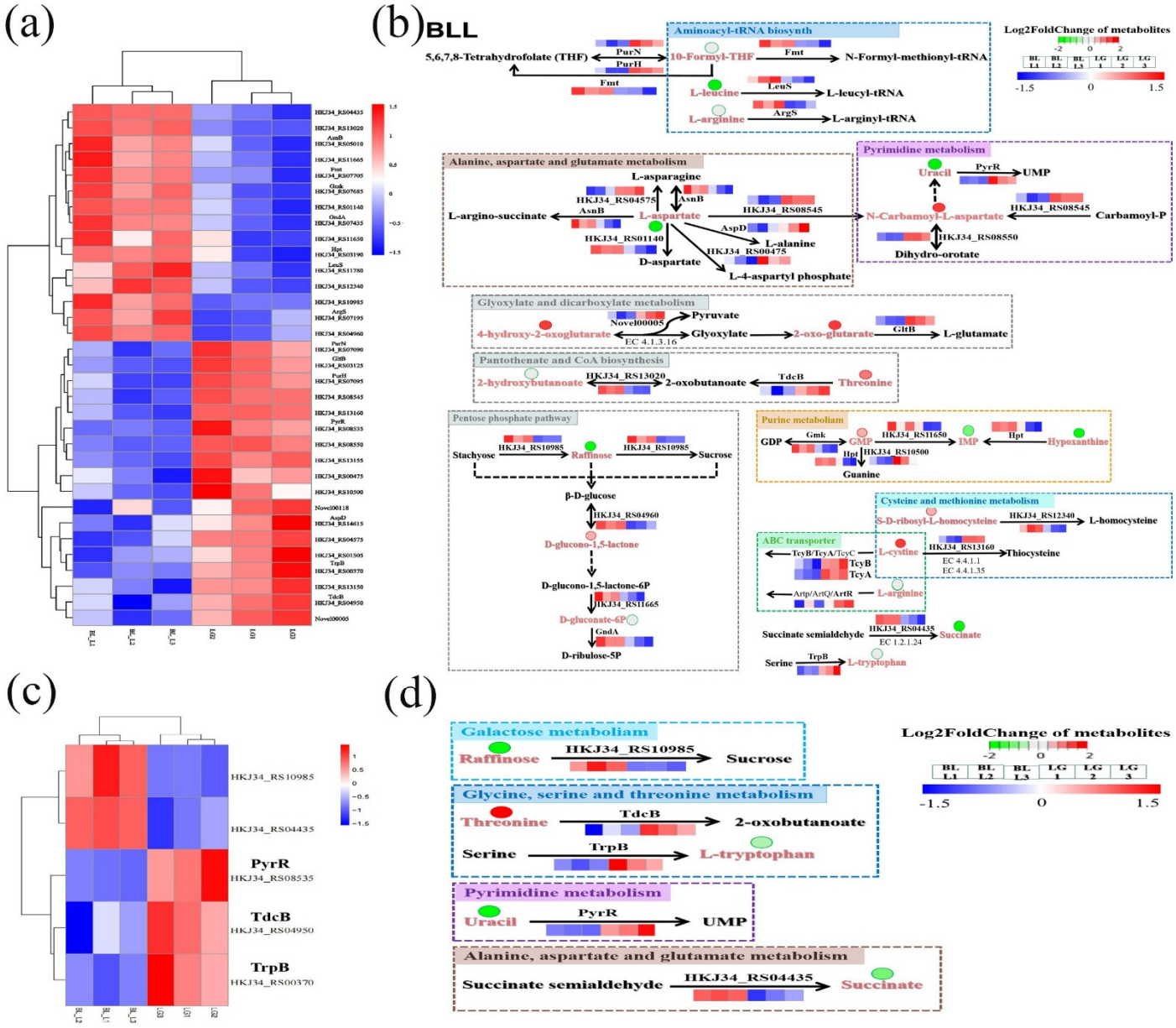

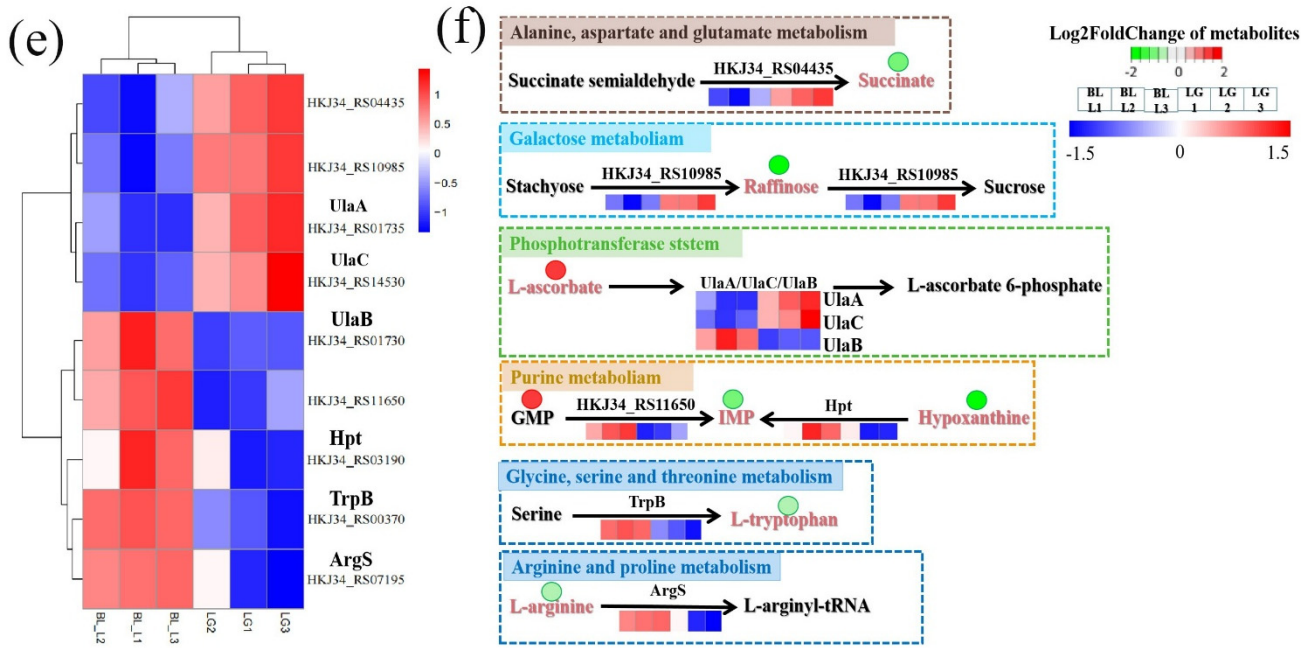

Fig 7: Schematic diagram of the backbone pathways for the biosynthesis of several bioactive compounds and the expression of key genes in BL versus L. The heatmap shows the level of gene expression (calculated using Log_2Fold Change, based on transcriptome data) (a), differential genes expression associated with bacterial growth (c) and functional activity (e) from red (higher expression) to blue (lower expression); The backbone pathways for the biosynthesis of several bioactive compounds and the expression of key genes (b), metabolic pathways associated with bacterial growth (d) and functional activity (f). The red color represents upregulation and blue color represents downregulation.

Thus, enzymes converted precursors with low bioactivity via transformation reactions to generate corresponding products with high bioactivity. And we hypothesized that enzyme-encoding genes are positively regulated when the change trends are consistent with those of differential metabolites, and genes exhibiting trends opposite to their change trends are negatively regulated genes. Nevertheless, the detailed mechanisms underlying specific biotransformations and the transforming enzymes are yet to be unraveled and warrant further investigations.

3.6 Cooperation between B.an3 and L.cp29

3.6.1 Impact of cooperation between B.an3 and L.cp29 on growth

Collectively, strains of the co-culture fermentation metabolized and produced different growth-promoting markers (Fig. 8). When compared with the metabolites produced by *L. paracasei* YL-29, those produced through co-culturing included L-thymidine, which is involved in nucleotide metabolism, and raffinose and stachyose, which are involved in galactose metabolism. L-tryptophan's role in neurotransmitter biosynthesis modulates gut-brain communication and immune responses in host-microbe interactions. These processes are fundamental for the growth and proliferation of bacteria in the co - culture system, contributing to the overall stability and functionality of the microbial community [65]. Moreover, when compared with the metabolites produced by *B. animalis* subsp. *lactis* HN-3, those produced through co-culturing included L-theronine, inosine, L-phenylalanine, L-tryptophan, succinic acid, and uracil, which are chiefly involved in nucleotide metabolism. Interestingly, an interaction was observed between L.cp29 and B.an3 through co-culture fermentation. Raffinose and stachyose utilization was found to be more significant in the presence

of L.cp29, but not manifested during B.an3 fermentation. The raffinose and stachyose contents were significantly reduced in the co-culture fermentation, possibly because they were converted to low-molecular-weight fructo-oligosaccharides, galacto-oligosaccharides, and mannan oligosaccharides and then used as prebiotics during the co-culture fermentation. Furthermore, fructooligosaccharides and galacto-oligosaccharides were used by B.an3, thereby promoting bacterial growth [66].

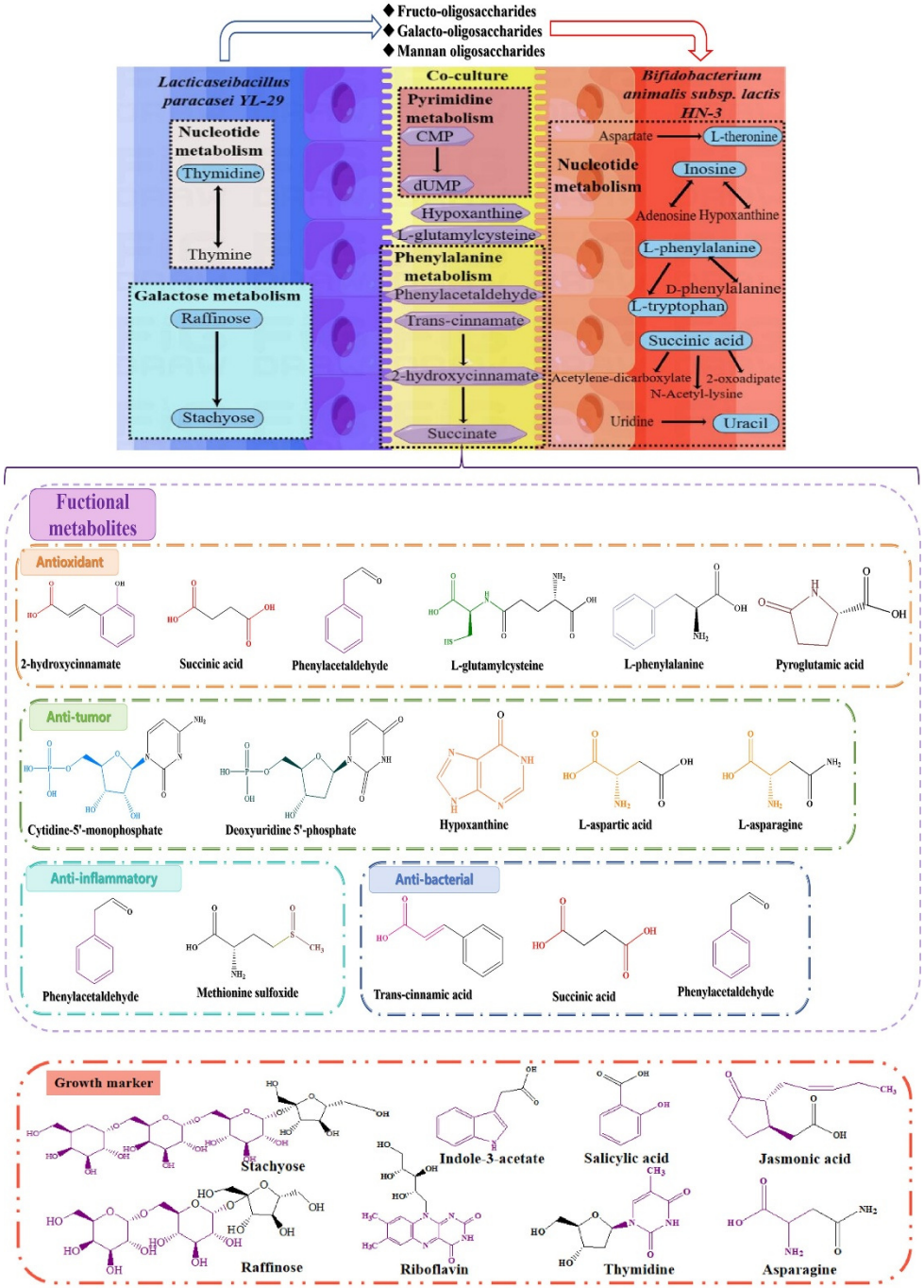

Fig 8: The mechanism of mutual promotion between B.an3 and L.cp29. The shape of blue: downregulated metabolites that are growth markers and functional substances in the fermented EWSJ; the shape of purple: metabolites of enhancing the functional activity of the EWSJ. Dark blue color indicates enzymes released by *Lacticaseibacillus paracasei* YL-29, red color indicates enzymes released by *Bifidobacterium animalis* subsp. *lactis* HN-3, and purple color indicates enzymes released by co-culture. The different shapes represent different kinds of enzymes, including hydrolases, racemases, proteinases, glycosidases, phosphatases, kinases, transferases, synthetases, permeases, lyases, dehydrogenases, reductases, asparaginases, aldolases, and transporters.

3.6.2 Impact function of cooperation between B.an3 and L.cp29

During co-culture fermentation, diverse transforming enzymes modified precursor structures, thereby producing products with better functional activities. These products were predominantly involved in pyrimidine metabolism, purine metabolism, amino acid biosynthesis, and phenylalanine metabolism. Of these, the contents of methionine sulfoxide, CMP, L-glutamylcysteine, phenylacetaldehyde, and trans-cinnamic acid, significantly increased and their functional activities also increased significantly. This effect was mainly reflected through the increase in the antioxidant, anti-inflammatory, antibacterial, and antitumor activities of these metabolites [67]. Methionine sulfoxide accumulation indicates robust cellular responses to anti - inflammatory [68]. Accordingly, we speculated that a cooperation-beneficial relationship exists between the monoculture and co-culture approaches. However, the roles of transforming enzymes and detailed mechanisms underpinning specific biotransformation and interactions remain unclear, warranting further investigations.

4. Conclusion

The interaction between B.an3 and L.cp29 fermentations was elucidated through the comprehensive analysis of significant changes in the levels of differential metabolites and the expressions of differential genes. Metabolomic and transcriptomic analyses revealed that raffinose and stachyose utilization were more significant in the presence of L.cp29, whereas raffinose utilization was more significant in the presence of B.an3. The raffinose and stachyose contents in the co-culture fermentation were significantly reduced and may be converted to fructo-oligosaccharides, galacto-oligosaccharides, and mannan oligosaccharide to serve as prebiotics. Furthermore, fructo-oligosaccharides and galacto-oligosaccharides can be further used by B.an3, which promotes bacterial growth. Under co-culture fermentation, the carbon source in EWSJ can be used more efficiently to produce greater numbers of growth-promoting profiles. L-thymidine, raffinose, stachyose, L-threonine, inosine, L-phenylalanine, L-tryptophan, succinic acid, and uracil were significantly decreased through galactose metabolism, amino acid biosynthesis, and nucleotide metabolism, which led to a better growth state in the co-culture fermentation than in the monoculture fermentation. On the other hand, some metabolites with strong functional activities (namely succinic acid, phenylacetaldehyde, L-glutamylcysteine, 2-hydroxycinnamate, CMP, dUMP, hypoxanthine, and trans-cinnamic acid) require more transformation in the co-culture fermentation than in the mono-culture fermentations through purine metabolism, pyrimidine metabolism, phenylalanine metabolism, and amino acid biosynthesis. The co-culture fermentation further converted bioactive components in EWSJ into bioactive metabolites, which possessed greater bioactivity, thereby laying the foundation for developing probiotic plant products. These metabolites can be used in food processing practices or as ingredients with improved health-promoting properties.

Conflict of interest

The authors declared that they have no conflict of interest.

Fundings

The research was supported by the National Natural Science Foundation of China (grant no. 32260568).

References

[1] Wang, M.; Zhang, Z.; Sun, H.; He, S.; Liu, S.; Zhang, T.; Wang, L.; Ma, G., Research progress of anthocyanin prebiotic activity: A review. Phytomedicine (2022), *102*, 154145. https://doi.org/10.1016/j.phymed.2022.154145

[2] Henrick, B. M.; Rodriguez, L.; Lakshmikanth, T.; Pou, C.; Henckel, E.; Arzoomand, A.; Olin, A.; Wang, J.; Mikes, J.; Tan, Z.; Chen, Y.; Ehrlich, A. M.; Bernhardsson, A. K.; Mugabo, C. H.; Ambrosiani, Y.; Gustafsson, A.; Chew, S.; Brown, H. K.; Prambs, J.; Bohlin, K.; Mitchell, R. D.; Underwood, M. A.; Smilowitz, J. T.; German, J. B.; Frese, S. A.; Brodin, P., Bifidobacteria-mediated immune system imprinting early in life. Cell (2021), *184* (15), 3884-3898 e11. https://doi.org/10.1016/j.cell.2021.05.030

[3] Wu, Y.; Li, S.; Tao, Y.; Li, D.; Han, Y.; Show, P. L.; Wen, G.; Zhou, J., Fermentation of blueberry and blackberry juices using Lactobacillus plantarum, Streptococcus thermophilus and Bifidobacterium bifidum: Growth of probiotics, metabolism of phenolics, antioxidant capacity in vitro and sensory evaluation. Food chemistry (2021), *348*, 129083. https://doi.org/10.1016/j.foodchem.2021.129083

[4] Araujo Rodrigues, T. J.; Albuquerque, A. P.; Silva de Azevedo, A. V.; da Silva, L. R.; de Bittencourt Pasquali, M. A.; de Araujo, G. T.; Monteiro, S. S.; Leite Lima, W. D.; Trindade Rocha, A. P., Production and Shelf-Life Study of Probiotic Caja (Spondias mombin L.) Pulp Using Bifidobacterium animalis ssp. Lactis B94. FOODS (2022), *11* (13). https://doi.org/10.3390/foods11131838

[5] Sakanaka, M.; Gotoh, A.; Yoshida, K.; Odamaki, T.; Koguchi, H.; Xiao, J. Z.; Kitaoka, M.; Katayama, T., Varied Pathways of Infant Gut-Associated Bifidobacterium to Assimilate Human Milk Oligosaccharides: Prevalence of the Gene Set and Its Correlation with Bifidobacteria-Rich Microbiota Formation. Nutrients (2019), *12* (1). https://doi.org/10.3390/nu12010071

[6] Havas, P.; Kun, S.; Styevkó, G.; Slačanac, V.; Hardi, J.; Rezessy-Szabó, J., Fruit and vegetable juice fermentation with Bifidobacteria. Acta Alimentaria (2014), *43* (Supplement 1), 64-72. https://doi.org/10.1556/Aalim.2014.4444

[7] Renye, J. A., Jr.; White, A. K.; Hotchkiss, A. T., Jr., Identification of Lactobacillus Strains Capable of Fermenting Fructo-Oligosaccharides and Inulin. Microorganisms (2021), *9* (10). https://doi.org/10.3390/microorganisms9102020

[8] Oliveira, W. A.; Rodrigues, A. R. P.; Oliveira, F. A.; Oliveira, V. S.; Laureano-Melo, R.; Stutz, E. T. G.; Lemos Junior, W. J. F.; Paula, B. P.; Esmerino, E. A.; Corich, V.; Giacomini, A.; Rodrigues, P.; Luchese, R. H.; Guerra, A. F., Potentially probiotic or postbiotic pre-converted nitrite from celery produced by an axenic culture system with probiotic lacticaseibacilli strain. Meat science (2021), *174*, 108408. https://doi.org/10.1016/j.meatsci.2020.108408

[9] Kwaw, E.; Ma, Y.; Tchabo, W.; Apaliya, M. T.; Wu, M.; Sackey, A. S.; Xiao, L.; Tahir, H. E., Effect of lactobacillus strains on phenolic profile, color attributes and antioxidant activities of lactic-acid-fermented mulberry juice. Food chemistry (2018), *250*, 148-154. https://doi.org/10.1016/j.foodchem.2018.01.009

[10] Maftei, N.-M.; Bogdan, R. E. G.; Boev, M.; Marin, D. B.; Ramos-Villarroel, A. Y.; Iancu, A.-V., Innovative Fermented Soy Drink with the Sea Buckthorn Syrup and the Probiotics Co-Culture of Lactobacillus Paracasei ssp. Paracasei (L. Casei® 431) and Bifidobacterium Animalis ssp. Lactis (Bb-12®). FERMENTATION-BASEL (2023), *9* (9). https://doi.org/10.3390/fermentation9090806

[11] Guo, S.; Li, B.; Wang, D.; Li, L.; Chen, Y.; Menghe, B., Metabolomic analysis of cooperative adaptation between Co-cultured Lacticaseibacillus casei Zhang and Lactiplantibacillus plantarum P8. Lwt (2022), *170*. https://doi.org/10.1016/j.lwt.2022.114105

[12] Peng, X. Y.; Wu, J. T.; Shao, C. L.; Li, Z. Y.; Chen, M.; Wang, C. Y., Co-culture: stimulate the metabolic potential and explore the molecular diversity of natural products from microorganisms. Mar Life Sci Technol (2021), *3* (3), 363-374. https://doi.org/10.1007/s42995-020-00077-5

[13] Soundharrajan, I.; Yoon, Y. H.; Muthusamy, K.; Jung, J. S.; Lee, H. J.; Han, O. K.; Choi, K. C., Isolation of Lactococcus lactis from Whole Crop Rice and Determining Its Probiotic and Antimicrobial Properties towards Gastrointestinal Associated Bacteria. Microorganisms (2021), *9* (12). https://doi.org/10.3390/microorganisms9122513

[14] Chen, Y.; Huang, Y.; Bai, Y.; Fu, C.; Zhou, M.; Gao, B.; Wang, C.; Li, D.; Hu, Y.; Xu, N., Effects of mixed cultures of Saccharomyces cerevisiae and Lactobacillus plantarum in alcoholic fermentation on the physicochemical and sensory properties of citrus vinegar. Lwt (2017), *84*, 753-763. https://doi.org/10.1016/j.lwt.2017.06.032

[15] Wang, A.; Guan, C.; Wang, T.; Mu, G.; Tuo, Y., Changes in Intracellular and Extracellular Metabolites of Mixed Lactobacillus Strains Enhance Inhibition of Pathogenic Bacterial Growth and Lipopolysaccharide-Induced Alleviation of RAW264.7 Cellular Inflammation. Probiotics Antimicrob Proteins (2023). https://doi.org/10.1007/s12602-023-10132-z

[16] Wang, S. Y.; Huang, R. F.; Ng, K. S.; Chen, Y. P.; Shiu, J. S.; Chen, M. J., Co-Culture Strategy of Lactobacillus kefiranofaciens HL1 for Developing Functional Fermented Milk. Foods (2021), *10* (9). https://doi.org/10.3390/foods10092098

[17] Garrigues, C.; Johansen, E.; Crittenden, R., Pangenomics--an avenue to improved industrial starter cultures and probiotics. Current opinion in biotechnology (2013), *24* (2), 187-91. https://doi.org/10.1016/j.copbio.2012.08.009

[18] Wang, X.; Feng, H.; Wang, Y.; Wang, M.; Xie, X.; Chang, H.; Wang, L.; Qu, J.; Sun, K.; He, W.; Wang, C.; Dai, C.; Chu, Z.; Tian, C.; Yu, N.; Zhang, X.; Liu, H.; Wang, E., Mycorrhizal symbiosis modulates the rhizosphere microbiota to promote rhizobia-legume symbiosis. MOLECULAR PLANT (2021), *14* (3), 503-516. https://doi.org/10.1016/j.molp.2020.12.002

[19] Cenci-Goga, B. T.; Sechi, P.; Iulietto, M. F.; Amirjalali, S.; Barbera, S.; Karama, M.; Aly, S. S.; Grispoldi, L., Characterization and Growth under Different Storage Temperatures of Ropy Slime-Producing *Leuconostoc mesenteroides* Isolated from Cooked Meat Products. JOURNAL OF FOOD PROTECTION (2020), *83* (6), 1043-1049. https://doi.org/10.4315/JFP-19-521

[20] Wang, C.; Wang, Y.; Teng, Y.; Zhang, Y., Win-win cooperation between plant substrates and probiotics: Revealing biotransformation and bioactive metabolites in Elaeagnus moorcroftii Wall. ex Schlecht fermented by Lacticaseibacillus paracasei YL-29. LWT (2024), *204*, 116442. https://doi.org/https://doi.org/10.1016/j.lwt.2024.116442

[21] Wen, B.; Mei, Z.; Zeng, C.; Liu, S., metaX: a flexible and comprehensive software for processing metabolomics data. BMC BIOINFORMATICS (2017), *18*. https://doi.org/10.1186/s12859-017-1579-y

[22] Shi, K.; Li, J.; Lv, J.; Liu, P.; Li, J.; Li, S., Full-length transcriptome sequences of ridgetail white prawn Exopalaemon carinicauda provide insight into gene expression dynamics during thermal stress. SCIENCE OF THE TOTAL ENVIRONMENT (2020), *747*. https://doi.org/10.1016/j.scitotenv.2020.141238

[23] Shao, L.; Li, T.; Yang, S.; Ma, L.; Cai, B.; Jia, Q.; Jiang, H.; Bai, T.; Li, Y., The prebiotic effects of fructooligosaccharides enhance the growth characteristics of Staphylococcus epidermidis and enhance the inhibition of Staphylococcus aureus biofilm formation. Int J Cosmet Sci (2024). https://doi.org/10.1111/ics.13020

[24] Lizardo, R. C. M.; Cho, H. D.; Won, Y. S.; Seo, K. I., Fermentation with mono- and mixed cultures of Lactobacillus plantarum and L. casei enhances the phytochemical content and biological activities of cherry silverberry (Elaeagnus multiflora Thunb.) fruit. Journal of the science of food and agriculture (2020), *100* (9), 3687-3696. https://doi.org/10.1002/jsfa.10404

[25] Wang, Y.; Wang, C.; Lan, Z.; Teng, Y.; Ni, Y.; Zhang, Y., The Biotransformation and Influence on the Functional Activities of Metabolites during the Fermentation of Elaeagnus moorcroftii Wall.ex Schlecht. Juice by Bifidobacterium animalis subsp. lactis HN-3. Foods (2024), *13* (6). https://doi.org/10.3390/foods13060926

[26] Engevik, M. A.; Luck, B.; Visuthranukul, C.; Ihekweazu, F. D.; Engevik, A. C.; Shi, Z.; Danhof, H. A.; Chang-Graham, A. L.; Hall, A.; Endres, B. T.; Haidacher, S. J.; Horvath, T. D.; Haag, A. M.; Devaraj, S.; Garey, K. W.; Britton, R. A.; Hyser, J. M.; Shroyer, N. F.; Versalovic, J., Human-Derived Bifidobacterium dentium Modulates the Mammalian Serotonergic System and Gut–Brain Axis. Cellular and Molecular Gastroenterology and Hepatology (2021), *11* (1), 221-248. https://doi.org/10.1016/j.jcmgh.2020.08.002

[27] Qiao, L.; Dou, X.; Song, X.; Chang, J.; Pi, S.; Zhang, X.; Zhu, L.; Zeng, X.; Xu, C., Protective effect of biogenic selenium nanoparticles against diquat-induced acute toxicity via regulation of gut microbiota and its metabolites. Food Chem Toxicol (2022), *170*, 113480. https://doi.org/10.1016/j.fct.2022.113480

[28] Duboux, S.; Pruvost, S.; Joyce, C.; Bogicevic, B.; Muller, J. A.; Mercenier, A.; Kleerebezem, M., The Pleiotropic Effects of Carbohydrate-Mediated Growth Rate Modifications in Bifidobacterium longum NCC 2705. Microorganisms (2023), *11* (3). https://doi.org/10.3390/microorganisms11030588

[29] Liang, Z.; Zheng, K.; Xie, G.; Luo, X.; Li, H., Sugar Utilization-Associated Food-Grade Selection Markers in Lactic Acid Bacteria and Yeast. Pol J Microbiol (2024), *73* (1), 3-10. https://doi.org/10.33073/pjm-2024-011

[30] Wu, J.; Yan, X.; Weng, P.; Chen, G.; Wu, Z., Homology- and cross-resistance of Lactobacillus plantarum to acid and osmotic stress and the influence of induction conditions on its proliferation by RNA-Seq. J Basic Microbiol (2021), *61* (6), 576-590. https://doi.org/10.1002/jobm.202100051

[31] Wenkang, H.; Jingui, L.; Wei, Z.; Jiangli, W.; Zhengbin, Y.; Furong, Z.; Xuefeng, Z., Multi-omics analysis reveals the microbial interactions of S. cerevisiae and L. plantarum on Suanyu, Chinese traditional fermented fish. Food research international (Ottawa, Ont.) (2023), *174* (Pt 1), 113525. https://doi.org/10.1016/j.foodres.2023.113525

[32] Shi, J.; Xia, C.; Tian, Q.; Zeng, X.; Wu, Z.; Guo, Y.; Pan, D., Untargeted metabolomics based on LC–MS to elucidate the mechanism underlying nitrite degradation by Limosilactobacillus fermentum RC4. Lwt (2022), *163*. https://doi.org/10.1016/j.lwt.2022.113414

[33] Ha, E. M., Escherichia coli-Derived Uracil Increases the Antibacterial Activity and Growth Rate of Lactobacillus plantarum. J Microbiol Biotechnol (2016), *26* (5), 975-87. https://doi.org/10.4014/jmb.1601.01063

[34] Elango, D.; Rajendran, K.; Van der Laan, L.; Sebastiar, S.; Raigne, J.; Thaiparambil, N. A.; El Haddad, N.; Raja, B.; Wang, W.; Ferela, A.; Chiteri, K. O.; Thudi, M.; Varshney, R. K.; Chopra, S.; Singh, A.; Singh, A. K., Raffinose Family Oligosaccharides: Friend or Foe for Human and Plant Health? FRONTIERS IN PLANT SCIENCE (2022), *13*. https://doi.org/10.3389/fpls.2022.829118

[35] Jiang, J.; Pavlova, N. N.; Zhang, J., Asparagine, a critical limiting metabolite during glutamine starvation. Molecular & cellular oncology (2018), *5* (3), e1441633-e1441633. https://doi.org/10.1080/23723556.2018.1441633

[36] Moran-Diez, M. E.; Tranque, E.; Bettiol, W.; Monte, E.; Hermosa, R., Differential Response of Tomato Plants to the Application of Three Trichoderma Species When Evaluating the Control of Pseudomonas syringae Populations. PLANTS-BASEL (2020), *9* (5). https://doi.org/10.3390/plants9050626

[37] Singh, K.; Gupta, R.; Shokat, S.; Iqbal, N.; Kocsy, G.; Perez-Perez, J. M.; Riyazuddin, R., Ascorbate, plant hormones and their interactions during plant responses to biotic stress. PHYSIOLOGIA PLANTARUM (2024), *176* (4). https://doi.org/10.1111/ppl.14388

[38] Jayaraman, S.; Kannan, M. A.; Rajendhran, N.; John, G. J.; Ramasamy, T., Indole-3-acetic acid impacts biofilm formation and virulence production of Pseudomonas aeruginosa. BIOFOULING (2023), *39* (8), 800-815. https://doi.org/10.1080/08927014.2023.2269537

[39] Solopova, A.; Bottacini, F.; Venturi degli Esposti, E.; Amaretti, A.; Raimondi, S.; Rossi, M.; van Sinderen, D., Riboflavin Biosynthesis and Overproduction by a Derivative of the Human Gut CommensalBifidobacterium longumsubsp.infantisATCC 15697. FRONTIERS IN MICROBIOLOGY (2020), *11*. https://doi.org/10.3389/fmicb.2020.573335

[40] Hatano, A.; Matsuzaka, R.; Shimane, G.; Wakana, H.; Suzuki, K.; Nishioka, C.; Kojima, A.; Kidowaki, M., Introduction of pseudo-base benzimidazole derivatives into nucleosides via base exchange by a nucleoside metabolic enzyme. Bioorg Med Chem (2023), *91*, 117411. https://doi.org/10.1016/j.bmc.2023.117411

[41] Lee, Y.-J.; Dai, N.; Muller, S. I.; Guan, C.; Parker, M. J.; Fraser, M. E.; Walsh, S. E.; Sridar, J.; Mulholland, A.; Nayak, K.; Sun, Z.; Lin, Y.-C.; Comb, D. G.; Marks, K.; Gonzalez, R.; Dowling, D. P.; Bandarian, V.; Saleh, L.; Correa, I. R.; Weigele, P. R., Pathways of thymidine hypermodification. NUCLEIC ACIDS RESEARCH (2022), *50* (6), 3001-3017. https://doi.org/10.1093/nar/gkab781

[42] Qiu, M.; Jiang, J.; Jiang, W.; Zhang, W.; Jiang, Y.; Xin, F.; Jiang, M., The biosynthesis of L-phenylalanine-derived compounds by engineered microbes. BIOTECHNOLOGY ADVANCES (2024), *77*. https://doi.org/10.1016/j.biotechadv.2024.108448

[43] Koo, B.; Choi, J.; Yang, C.; Nyachoti, C. M., Diet complexity and L-threonine supplementation: effects on growth performance, immune response, intestinal barrier function, and microbial metabolites in nursery pigs. JOURNAL OF ANIMAL SCIENCE (2020), *98* (5). https://doi.org/10.1093/jas/skaa125

[44] Cui, L.; Ma, R.; Cai, J.; Guo, C.; Chen, Z.; Yao, L.; Wang, Y.; Fan, R.; Wang, X.; Shi, Y., RNA modifications: importance in immune cell biology and related diseases. SIGNAL TRANSDUCTION AND TARGETED THERAPY (2022), *7* (1). https://doi.org/10.1038/s41392-022-01175-9

[45] Kaushik, M. S.; Pati, S. R.; Soni, S.; Mishra, A.; Sushmita, K.; Kateriya, S., Establishment of Optogenetic Modulation of cAMP for Analyzing Growth, Biofilm Formation, and Virulence Pathways of Bacteria Using a Light-Gated Cyclase. APPLIED SCIENCES-BASEL (2020), *10* (16). https://doi.org/10.3390/app10165535

[46] Stein, B. W.-L. A. O. P. F. J. V. B. K. T., Gramicidin S synthetase 1 (phenylalanine racemase), a prototype of amino acid racemases containing the cofactor 4'-phosphopantetheine. Biochemistry (1995), *34* (14), 4633-4642. https://doi.org/ https://doi.org/10.1021/bi00014a017

[47] Chandel, N. S., Nucleotide Metabolism. Cold Spring Harb Perspect Biol (2021), *13* (7). https://doi.org/10.1101/cshperspect.a040592

[48] Nwosu, Z. C.; Ward, M. H.; Sajjakulnukit, P.; Poudel, P.; Ragulan, C.; Kasperek, S.; Radyk, M.; Sutton, D.; Menjivar, R. E.; Andren, A.; Apiz-Saab, J. J.; Tolstyka, Z.; Brown, K.; Lee, H.-J.; Dzierozynski, L. N.; He, X.; Hari, P. S.; Ugras, J.; Nyamundanda, G.; Zhang, L.; Halbrook, C. J.; Carpenter, E. S.; Shi, J.; Shriver, L. P.; Patti, G. J.; Muir, A.; Pasca di Magliano, M.; Sadanandam, A.; Lyssiotis, C. A., Uridine-derived ribose fuels glucose-restricted pancreatic cancer. NATURE (2023), *618* (7963), 151-+. https://doi.org/10.1038/s41586-023-06073-w

[49] Rolfo, C.; Giovannetti, E.; Martinez, P.; McCue, S.; Naing, A., Applications and clinical trial landscape using Toll-like receptor agonists to reduce the toll of cancer. NPJ Precis Oncol (2023), *7* (1), 26. https://doi.org/10.1038/s41698-023-00364-1

[50] Ng, K. R.; Lyu, X.; Mark, R.; Chen, W. N., Antimicrobial and antioxidant activities of phenolic metabolites from flavonoid-producing yeast: Potential as natural food preservatives. Food chemistry (2019), *270*, 123-129. https://doi.org/10.1016/j.foodchem.2018.07.077

[51] Wang, S.; Kang, O.-H.; Kwon, D.-Y., Trans-Cinnamaldehyde Exhibits Synergy with Conventional Antibiotic against Methicillin-Resistant Staphylococcus aureus. INTERNATIONAL JOURNAL OF MOLECULAR SCIENCES (2021), *22* (5). https://doi.org/10.3390/ijms22052752

[52] Zhang, B.; Jiang, X.; Huang, G.; Xin, X.; Attaribo, T.; Zhang, Y.; Zhang, N.; Gui, Z., Enhancement of Stability and Antioxidant Activity of Mulberry Anthocyanins Through Succinic Acid Acylation. Food Technol Biotechnol (2022), *60* (3), 321-329. https://doi.org/10.17113/ftb.60.03.22.7203

[53] Rabiej-Koziol, D.; Krzeminski, M. P.; Szydlowska-Czerniak, A., Synthesis of Steryl Hydroxycinnamates to Enhance Antioxidant Activity of Rapeseed Oil and Emulsions. MATERIALS (2020), *13* (20). https://doi.org/10.3390/ma13204536

[54] Anthamatten, L.; von Bieberstein, P. R.; Menzi, C.; Zund, J. N.; Lacroix, C.; de Wouters, T.; Leventhal, G. E., Stratification of human gut microbiomes by succinotype is associated with inflammatory bowel disease status. MICROBIOME (2024), *12* (1). https://doi.org/10.1186/s40168-024-01897-8

[55] Shakartalla, S. B.; Ashmawy, N. S.; Semreen, M. H.; Fayed, B.; Al Shareef, Z. M.; Jayakumar, M. N.; Ibrahim, S.; Rahmani, M.; Hamdy, R.; Soliman, S. S. M., ^{1}H-NMR metabolomics analysis identifies hypoxanthine as a novel metastasis-associated metabolite in breast cancer. SCIENTIFIC REPORTS (2024), *14* (1). https://doi.org/10.1038/s41598-023-50866-y

[56] Choe, E.; Min, D. B., Mechanisms of Antioxidants in the Oxidation of Foods. Comprehensive Reviews in Food Science and Food Safety (2009), *8* (4), 345-358. https://doi.org/10.1111/j.1541-4337.2009.00085.x

[57] Yerragunta, V. P., P.; Anusha, V.; KumaraSwamy, T.; Suman, S.; Samhitha, T, Pyrimidine and its biological activity: a review. PharmaTutor (2013), *1* (2), 39-44.

[58] Diaz-Munoz, M.; Hernandez-Munoz, R.; Butanda-Ochoa, A., Structure-activity features of purines and their receptors: implications in cell physiopathology. Mol Biomed (2022), *3* (1), 5. https://doi.org/10.1186/s43556-022-00068-1

[59] Song, J.; Liu, Y.; Yin, X.; Nan, Y.; Shi, Y.; Chen, X.; Liang, H.; Zhang, J.; Ma, B., Isolation and structural elucidation of prebiotic oligosaccharides from Ziziphi Spinosae Semen. Carbohydrate Research (2023), *534*, 108948. https://doi.org/https://doi.org/10.1016/j.carres.2023.108948

[60] Elango, D.; Rajendran, K.; Van der Laan, L.; Sebastiar, S.; Raigne, J.; Thaiparambil, N. A.; El Haddad, N.; Raja, B.; Wang, W.; Ferela, A.; Chiteri, K. O.; Thudi, M.; Varshney, R. K.; Chopra, S.; Singh, A.; Singh, A. K., Raffinose Family Oligosaccharides: Friend or Foe for Human and Plant Health? Front Plant Sci (2022), *13*, 829118. https://doi.org/10.3389/fpls.2022.829118

[61] Han, M.; Zhang, C.; Suglo, P.; Sun, S.; Wang, M.; Su, T., l-Aspartate: An Essential Metabolite for Plant Growth and Stress Acclimation. MOLECULES (2021), *26* (7). https://doi.org/10.3390/molecules26071887

[62] Lara-Cervantes, T. d. J.; Carrillo-Inungaray, M. L.; Balderas-Hernández, V. E.; Aguilar-Zárate, P.; Veana, F., (2022). https://doi.org/10.21203/rs.3.rs-1259500/v1

[63] Wang, J.; Bai, X.; Peng, C.; Yu, Z.; Li, B.; Zhang, W.; Sun, Z.; Zhang, H., Fermented milk containing Lactobacillus casei Zhang and Bifidobacterium animalis ssp. lactis V9 alleviated constipation symptoms through regulation of intestinal microbiota, inflammation, and metabolic pathways. Journal of Dairy Science (2020), *103* (12), 11025-11038. https://doi.org/https://doi.org/10.3168/jds.2020-18639

[64] Otten, A. T.; Bourgonje, A. R.; Peters, V.; Alizadeh, B. Z.; Dijkstra, G.; Harmsen, H. J. M., Vitamin C Supplementation in Healthy Individuals Leads to Shifts of Bacterial Populations in the Gut-A Pilot Study. ANTIOXIDANTS (2021), *10* (8). https://doi.org/10.3390/antiox10081278

[65] Gao, K.; Mu, C.-l.; Farzi, A.; Zhu, W.-y., Tryptophan Metabolism: A Link Between the Gut Microbiota and Brain. ADVANCES IN NUTRITION (2020), *11* (3), 709-723. https://doi.org/10.1093/advances/nmz127

[66] You, S.; Ma, Y.; Yan, B.; Pei, W.; Wu, Q.; Ding, C.; Huang, C., The promotion mechanism of prebiotics for probiotics: A review. Frontiers in nutrition (2022), *9*, 1000517. https://doi.org/10.3389/fnut.2022.1000517

[67] Lin, M.; Han, P.; Li, Y.; Wang, W.; Lai, D.; Zhou, L., Quinoa Secondary Metabolites and Their Biological Activities or Functions. Molecules (2019), *24* (13). https://doi.org/10.3390/molecules24132512

[68] Rey, P.; Tarrago, L., Physiological Roles of Plant Methionine Sulfoxide Reductases in Redox Homeostasis and Signaling. ANTIOXIDANTS (2018), *7* (9). https://doi.org/10.3390/antiox7090114